REPORT DOCUMENTATION PAGE

Form Approved
OMB No. 0704-0188

1. REPORT DATE *(DD-MM-YYYY)*	**2. REPORT TYPE**	**3. DATES COVERED** *(From - To)*
12-11-2020	Technical Report	May, 2019 - Oct, 2020

4. TITLE AND SUBTITLE

Impact of Exhaust Water Acidity on Nafion© Membrane Proton Conductivity at Operating Temperatures above 1000°C

5a. CONTRACT NUMBER

5b. GRANT NUMBER

5c. PROGRAM ELEMENT NUMBER

6. AUTHOR(S)

Theodore E. Burye

5d. PROJECT NUMBER

5e. TASK NUMBER

5f. WORK UNIT NUMBER

7. PERFORMING ORGANIZATION NAME(S) AND ADDRESS(ES)

US Army CCDC Ground Vehicle Systems Center (GVSC)
Ground Vehicle Power and Mobility (GVPM)
6501 E. 11 Mile Road
Warren, MI 48397

8. PERFORMING ORGANIZATION REPORT NUMBER

OPSEC 4777

9. SPONSORING / MONITORING AGENCY NAME(S) AND ADDRESS(ES)

US Army CCDC Ground Vehicle Systems Center (GVSC)
Ground Vehicle Power and Mobility (GVPM)
6501 E. 11 Mile Road
Warren, MI 48397

10. SPONSOR/MONITOR'S ACRONYM(S)

11. SPONSOR/MONITOR'S REPORT NUMBER(S)

12. DISTRIBUTION / AVAILABILITY STATEMENT

DISTRIBUTION A. Approved for public release; distribution unlimited. OPSEC# 4777.

13. SUPPLEMENTARY NOTES

14. ABSTRACT

15. SUBJECT TERMS

16. SECURITY CLASSIFICATION OF: Available for Public Release			**17. LIMITATION OF ABSTRACT**	**18. NUMBER OF PAGES**	**19a. NAME OF RESPONSIBLE PERSON**
a. REPORT	**b. ABSTRACT**	**c. THIS PAGE**	Same As Report (SAR)	45	Theodore Burye
UNCLAS	UNCLAS	UNCLAS			**19b. TELEPHONE NUMBER** *(include area code)* 586-282-3047

Impact of Exhaust Water Acidity on Nafion© Membrane Proton Conductivity at Operating Temperatures above 100^0C

Prepared by:

Dr. Theodore Burye
Chemical Engineer
theodore.e.burye2.civ@mail.mil
Fuel Cell Technologies
Ground Vehicle Power and Mobility (GVPM)
Combat Capabilities Development Command (CCDC) Ground Vehicle System Center (GVSC)

Acknowledgements

The Electrochemical Impedance Spectroscopy (EIS) data was acquired from the Fuel Cell Laboratory located at the Ground Vehicle System Center (GVSC) in building 212B. Theodore Burye, from the Fuel Cell Technologies group, collected the EIS data.

The Scanning Electron Microscopy (SEM), Energy Dispersive Spectroscopy (EDS) and X-ray Diffraction (XRD) data were acquired from the Metallurgy laboratory located at the GVSC in building 200D. Demetrios Tzelepis, from the Characterization & Failure Analysis group, helped collect XRD data.

The Fourier-Transform Infrared (FTIR) Spectroscopy and Thermal Gravimetric Analysis (TGA) data were acquired from the Elastomer, Isomer, Polymer laboratory located at the GVSC in building 215. William Roland from the Characterization & Failure Analysis group, collected this data.

Table of Contents

List of Tables

List of Figures

1. Abbreviations List

CCDC: Combat Capabilities Development Command

EDS: Energy Dispersive Spectroscopy

EIS: Electrochemical Impedance Spectroscopy

FTIR: Fourier-Transform Infrared

GVSC: Ground Vehicle System Center

IC: Internal Combustion

PEM: Proton Exchange Membrane

PEMFC: Proton Exchange Membrane Fuel Cell

RH: Relative Humidity

SEM: Scanning Electron Microscopy

TGA: Thermo-Gravimetric Analysis

XRD: X-ray Diffraction

2. Introduction

Fuel cells are being looked at with more interest by the U.S. Army as next generation combat vehicles will require additional electrical power for additional roles. Some of these new roles include silent watch, next-generation sensors and jamming devices, vehicle exportable power and Warfighter-carried exportable power. Batteries would be a possible option to power vehicles for these roles, however, the number of batteries required for these various roles would use a large amount of space in each vehicle and it would be difficult to maintain charge. Fuel cells make a better choice and are capable of avoiding these issues. First, they can use energy-dense fuel (by using hydrocarbon fuel directly or through on-board reforming) which allows vehicles to operate for longer periods of time. Second, they are energy efficient so vehicles use less fuel and can operated for longer. Third, fuel cells and the fuel are energy-dense so they are capable of providing power required in a smaller space-claim over a longer period, thus saving precious space inside the vehicle.

Many papers and articles have previously mentioned that, while Proton Exchange Membrane Fuel Cells (PEMFCs) have the advantages listed above, they still have are susceptible to multiple issues which result lower the stack durability and performance. Some of these issues are operating temperature [1, 2, 3], internal electrical bias [4], catalyst particle size [5], and exhaust water conductivity [6], in addition to the well-known stack sealing and thermal cycling issues. Degradation caused by PEMFC elevated stack operating temperatures (>100°C) has been of interest to the U.S. Army due to combat vehicles having reduced heat rejection caused by reduced air flow through their ballistic grills. The impact of elevated operating temperatures has been previously investigated and reported on [7] to determine the impact on membrane proton transport and internal structural properties. In addition, the previous work on catalyst degradation [6] showed acetic acid, produced as a byproduct by the PEMFC, could be released into the exhaust water. That previous report focused on the catalyst degradation caused by the acetic acid, it did also cause the acidity of the exhaust water to increase which could also enhance the breakdown of membranes at elevated temperatures.

The purpose of this paper is to examine the impact acetic acid, added to exhaust water, had on the Nafion© membrane proton conductivity degradation behavior when heated at elevated operating temperatures. These results will be contrasted against Nafion© membrane proton conductivity degradation results after being heated using elevated operating temperatures, without acetic acid being added to the water. Multiple formulations of Nafion© exist such as 112, 211, 212, NE1035, 115, 117 and 1110, to name a few of the more common formulations. This report used Nafion© 115, 117 and 1110 (the three sample types will be referred to 115, 117 and 1110 for the remainder of this paper) for the following reasons:

1. 117 is a common formulation used throughout literature studies [8, 9, 10] and thus had relevance in the advancement of PEMFC materials.
2. One purpose of this report was to investigate the effects of membrane thickness when exposed to temperatures outside the recommended temperature operating range, while 115 and 1110 are thinner and thicker versions of 117, respectively.

The membrane materials were exposed to 21°C, 65°C, 120°C and 140°C for 2, 8 and 24 hours, in the presence of 16MΩ water mixed with 5 vol% acetic acid. The following sections of this report will compare changes in the proton conductivity using Electrochemical Impedance Spectroscopy (EIS).

3. Experimental Operating Conditions

3.1. Introduction

The following section describes the Nafion© membrane sample preparation, experimental setup and characterization techniques used for all temperatures and sample thickness used while saturated in acidic and distilled water solutions.

3.2. Sample Preparation

30 cm x 30 cm sheets of each membrane material were purchased from the Fuel Cell Store, https://www.fuelcellstore.com. These three materials were selected since all three have the same equivalent weight of 1100 but have different material thicknesses. Material thickness were 127 µm (115), 183 µm (117) and 254 µm (1110).

3.2.1. Room Temperature Baseline and Material Identification Measurements

To establish material identification and a baseline for each characterization technique measurements were initially recorded at room temperature (21°C). Room temperature measurements used two different sample sizes, depending on the characterization test being performed. The first sample size consisted of square samples, cut from each material sheet for each temperature, approximately 1.27 cm x 1.27 cm in surface area. The second sample size consisted of rectangular samples, cut from each material sheet for each material thickness, which were approximately 0.979 cm x 0.869 cm in surface area. The square samples were analyzed using the following characterization techniques.

1. EDS
2. TGA
3. SEM
4. Mass Change Measurements
5. Water Absorption Measurements
6. FTIR
7. XRD

The rectangular samples were analyzed using only the EIS characterization technique.

3.2.2. Elevated Heating & Acetic Acid Experiments

Elevated heating (65°C, 120°C and 140°C) experiments combined with acetic acid also used the 2.54 cm x 5.1 cm sample size since the following samples were characterized using only the EIS to compare changes in calculated proton conductivity.

3.3. Experimental Setup

The following experimental setup designs were used while heating each sample. The following information was not used for samples characterized for room temperature baseline measurements since those samples did not have an external heat source applied.

3.3.1. 65°C Heating Experimental Setup

Three 100 mL beakers, each containing 50 mL of a 5 vol% acetic acid solution were placed onto Corning PC-420D hotplates (Corning, Corning, NY, USA), shown in Figure 1 . The 5 vol% acetic acid solution was produced by mixing 16MΩ water and glacial acetic acid (Fisher Scientific, Waltham, MA, USA) in appropriate quantities. The hotplate set point was placed to 120°C which allowed the solution in each beaker to reach ~65°C. The acetic acid solution temperature was verified to be 65°C using an external thermocouple. Samples were submerged and heated in the 5 vol% acetic acid solution for 2, 8 and 24 hours. The samples heated for 2 and 8 hours were taken out of their respective water bath at the end of their experiment. Samples heated for 24 hours were heated for three 8 hour periods over three days, where the hot plate was turned off between each day and each sample was allowed to stay submerged in the water bath overnight between each day. The samples heated for 24 hours were then removed from their respective water baths at the end of the experiment.

After being heated all samples were placed into a Bel-Art Secadaor clear 2.0 auto-desiccator cabinet (Bel-Art – SP Scienceware, South Wayne, NJ, USA), shown in Figure 2. Each sample remained in the desiccator for at least 6 hours to bring the water content in each sample to a baseline level and also to allow each sample enough time to cool down to room temperature (21°C).

3.3.1. 120°C and 140°C Heating Experimental Setup

Samples heated to 120°C and 140°C were placed inside a Supercritical Fluid Technologies HPR-Micro Reactor (Supercritical Fluid Technologies, Newark, DE, USA) system, which sealed each sample from the ambient environment, shown in Figure 3. The sealed reactor maintained a constant internal volume which allowed the water temperature to exceed 100°C and simultaneously increase its pressure. In addition to the sample, 50 mL of 5 vol% acetic acid solution was placed inside the reactor. Heating each sample and solution was achieved by using a heating ring placed on the outside of the reactor chamber. A thermocouple was placed between the heating ring and outer wall of the reactor to control the temperature using the assigned se tpoint. A stir bar was also used, at a speed of ~400 RPM to increase heat distribution throughout the water bath. Samples were heated at 120°C or 140°C for 2, 8 or 24 hours. Previous measurements, using a thermocouple attached to the side of the reactor, showed a set point of 160°C was necessary to reach a water temperature of 120°C and a set point of 200°C was necessary to reach a water temperature of 140°C.

Figure 1: 65°C Hotplate and Beaker for Heating 115, 117 and 1110 Samples to 65°C

Figure 2: Auto-Desiccator used to Dry and Cool 115, 117 and 1110 Samples

Samples heated for 2 and 8 hours were first allowed to cool (to around 55°C) to reduce the pressure inside the reactor before opening it and removing each sample from the 5 vol% acetic acid solution. Samples heated for 24 hours were heated for three 8 hour periods over three days, where the heating ring was turned off at the end of each day and the reactor remained sealed and pressurized overnight between each day. At the completion of each 24 hour experiment the reactor was allowed to cool and then the reactor was opened and the samples were removed from the 5 vol% acetic acid.

After being removed from the reactor all samples were then placed into the auto-desiccator shown in Figure 2. Each sample remained in the desiccator for at least 6 hours to lower the water content in each sample to a baseline level and also to allow each sample enough time to cool down to room temperature (21°C).

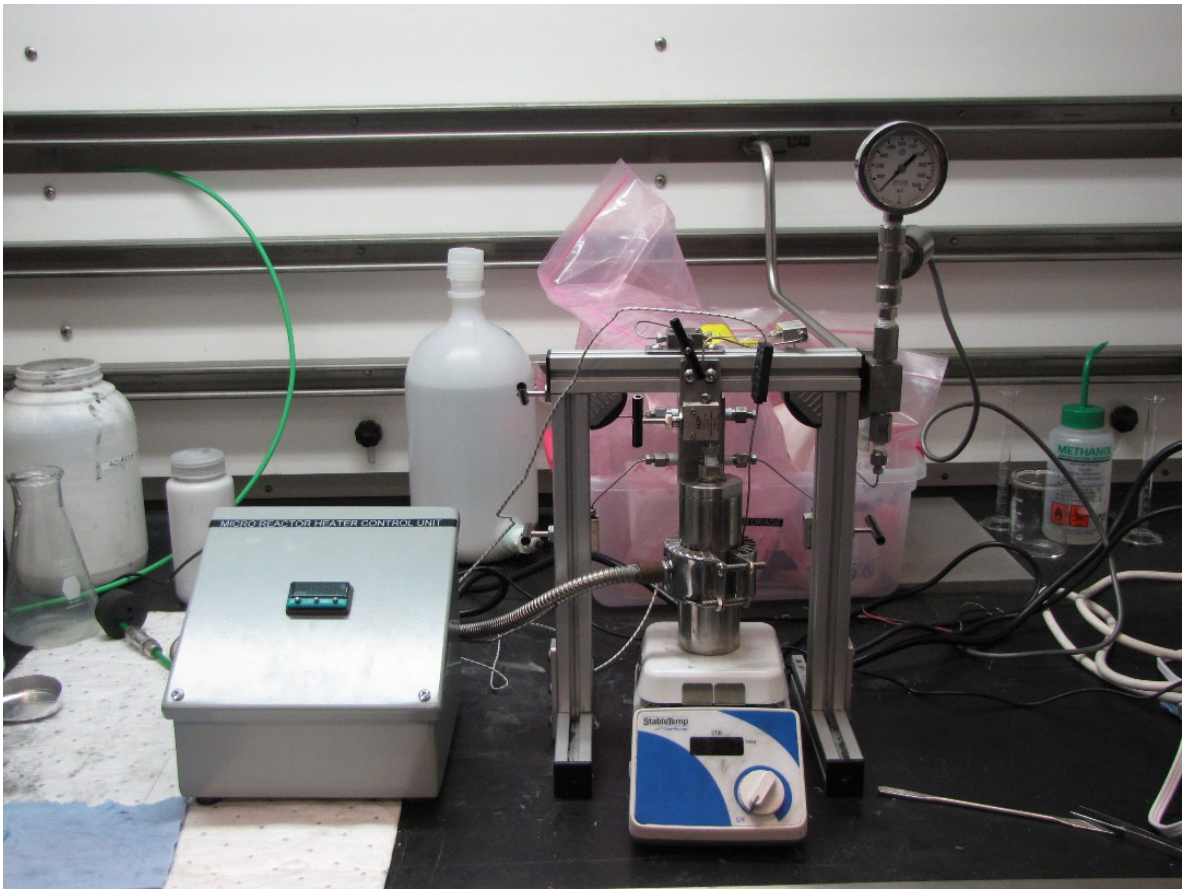

Figure 3: Reactor with Heating Ring and Stirbar System for Heating 115, 117 and 1110 Samples at 120°C and 140°C

3.4. Characterization Techniques

3.4.1. ThermoGravimetric Analysis (TGA)

ThermoGravimetric Analysis (TGA) was performed at the Elastomer, Isomer, Polymer laboratory located in building 215 at GVSC.

TGA was performed using a TA Instruments TGA Q5000 system (TA Instruments; New Castle, DE, USA). Between 10.00 mg and 12.00 mg of sample was placed in a platinum pan and was heated from 21°C to 700°C using a ramp rate of 30°C/min in a nitrogen atmosphere.

3.4.2. Scanning Electron Microscopy (SEM) and Electron Dispersive Spectroscopy (EDS)

Scanning Electron Microscopy (SEM) microscopy images and EDS analysis were performed at the Characterization & Failure Analysis group Metallurgy Laboratory located in building 200D at GVSC.

SEM was performed using a Hitachi system (Hitachi; Krefeld, Germany) with an electron voltage of 5.0kV, a magnification range of 2,000x, and a working distance of 10 mm. Energy Dispersive Spectroscopy (EDS) was performed using an Oxford Instruments system (Oxford Instruments; Concord, MA, USA) with an electron voltage of 30.0kV, a magnification range of 200x and a working distance of 10 mm.

3.4.3. X-Ray Diffraction (XRD)

X-Ray Diffraction (XRD) analysis were performed at the Characterization & Failure Analysis group Metallurgy Laboratory located in building 200D at GVSC.

XRD was performed using a SmartLab X-ray Diffraction (XRD) system (Rigaku Americas Corporation; The Woodlands, TX, USA). Broad material scans were conducted from $10° \leq 2\theta° \leq 90°$ with a 0.040 step, 1.00°/min scan speed, a copper filament and nickel filter, and at 20 kV.

3.4.4. Electrochemical Impedance Spectroscopy (EIS)

Electrochemical Impedance Spectroscopy (EIS) analysis were performed at the Fuel Cell Technologies group Fuel Cell Laboratory located in building 212B at GVSC.

EIS analysis was performed using a Solartron SI 1287 Electrochemical Interface interfaced with a Solartron 1255B Frequency Response Analyzer (Solartron Analytical, Farnborough, Hampshire, UK). EIS scans were performed using the 2-point method using a current sweep with no DC voltage, a current amplitude of 0.001A and a frequency range from 10^5 to 0.1 Hz.

3.4.5. Fourier-Transform Infrared Spectroscopy (FTIR)

Fourier-Transform Infrared (FTIR) analysis was performed at the Elastomer, Isomer, Polymer laboratory located in building 215 at GVSC.

FTIR analysis was performed using a Thermo Scientific Nicolet 6700 system (Thermo Scientific Instruments Corporation; Madison, WI, USA). FTIR scans were performed between 4000 and 675 cm^{-1} wavenumbers, using a Germanium crystal, 64 scans were performed per sample.

3.4.6. Mass Change Measurements

Mass change measurements were performed at the Fuel Cell Technologies group Fuel Cell Laboratory located in building 212B at GVSC.

Sample mass change measurements were determined using the following procedure. Samples, prior to being heated, cooled or frozen were first placed into the auto-desiccator for at least 6 hours to dry each sample so the relative humidity (RH) in the desiccator was <10% (referred to as "Dry" for the remainder of the paper). Each dry sample had its mass measured using a Mettler Toledo ML54T analytical balance with a 0.1 mg resolution (Mettler Toledo, Columbus, OH, USA), shown in Figure 4. Samples were then submerged in 16MΩ water for 1 hour to saturate each sample. Each sample, being dried after having different temperatures applied, had their mass measured again and compared to their original measured mass prior to each experiment. Mass changes were determined by subtracting the original sample mass from the post-experiment sample mass.

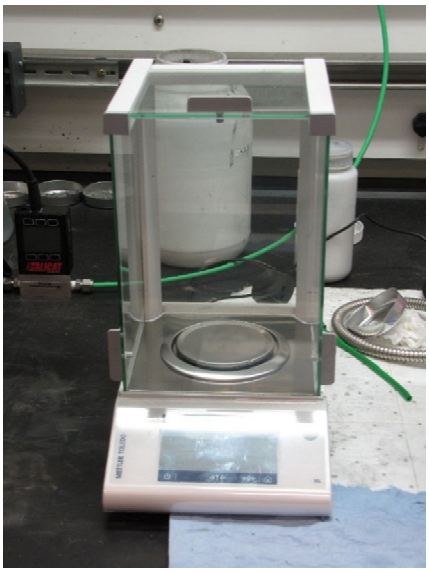

Figure 4: Mettler Toledo Analytic Balance for Dry and Saturated Sample Mass Measurements

3.4.7. Water Absorption Measurements

Water absorption measurements were performed at the Fuel Cell Technologies group Fuel Cell Laboratory located in building 212B at GVSC.

Sample water absorption measurements were determined using a similar method to the mass change measurements. The primary difference between these two characterization measurements is that this method also measures the saturated sample mass before and after experimentation in addition to the dry mass before and after experimentation. Samples, prior to being heated, cooled or frozen were first placed into the auto-desiccator for at least 6 hours to dry each sample so the RH in the desiccator was <10%. Each dry sample had its mass measured using the analytical balance. Samples were submerged in 16MΩ water for 1 hour to simulate a 100% RH environment (referred to as "Saturated" for the remainder of the paper), had their surface dried and then their saturated masses was measured. Samples then had various temperatures applied, had their surfaces dried and then placed into the auto-desiccator. After at least 6 hours in the desiccator the samples were removed, had their dry masses measured, and then were saturated again using 16MΩ water for 1 hour. Finally the post-experimentation saturated sample masses were recorded on the analytical balance. Sample water absorption measurements were determined before and after experimentation for each sample. Absorption measurements were calculated using the following formula in Equation 1:

$$Water\ Absorption\ \% = \frac{(Saturated\ Sample\ Mass - Dry\ Sample\ Mass)}{Dry\ Sample\ Mass} * 100 \quad [1]$$

Where,

Water Absorption % = % Water Absorbed by the Sample after being Submerged in Water for 1 hour on a Calculated using a Mass Basis

Saturated Samples Mass = Sample Mass after being Submerged in Water for 1 hour before or after experiments

Dry Sample Mass = Sample Mass after being Desiccator for at least 6 hours within a <10% RH Environment before or after experiments

3.4.8. Proton Conductivity Measurements

Proton conductivity measurements were performed at the Fuel Cell Technologies group Fuel Cell Laboratory located in building 212B at GVSC.

Rectangular samples were punched, using a hammer punch, from sample pieces submerged in 16 MΩ water or 5 vol% acetic acid solution. Unheated (21°C) and heated samples (65°C, 120°C and 140°C) all had their proton conductivity tested after experimentation. The shape of the punched sample is shown in Figure 5 below. The sample length (*L*) and width (*W*) were constant values of 0.979 cm and 0.869 cm, respectively. Sample thickness (*H*) for dry and saturated samples, before and after experimentation, was also measured using a caliper and then recorded. Collected raw EIS impedance data was plotted for each punched sample, where the impedance imaginary component was on the y-axis and the impedance real

component was on the x-axis producing a Nyquist plot. The ohmic resistance (*R*) (distance between the origin and the first x-axis intercept) for proton conduction through the membrane was calculated from each sample Nyquist plot. Proton conductivity measurements were then calculated using the length, width and thickness sample measurements and resistance calculations from each Nyquist plot in Equations 2 and 3 below:

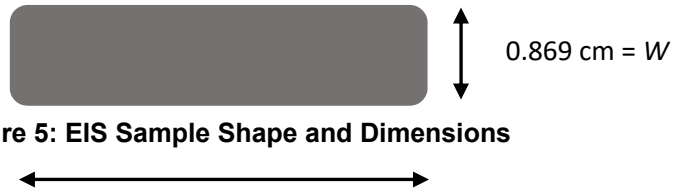

Figure 5: EIS Sample Shape and Dimensions

$$\sigma = \frac{1}{\rho} = \frac{L}{R*A} \quad [2]$$

$$A = H * W \quad [3]$$

Where,

σ = Calculated proton conductivity through the sample (S/cm)

ρ = Calculated proton transport resistivity through the sample (Ω*cm)

L = Sample length (0.979 cm)

R = Calculated ohmic resistance between the origin and initial x-axis intercept on the Nyquist plot (Ω)

A = Calculated proton transport cross-sectional area (cm^2)

H = Sample thickness (µm)

W = Sample width (0.869 cm)

4. Baseline Measurements

4.1. Introduction

This section will show baseline measurements for 115, 117 and 1110 before any operating temperatures above or below ambient were applied. Samples were not saturated (referred to as dry) when characterized, unless otherwise stated (referred to as saturated), such as the water absorption and EIS characterization measurements. The relative humidity and temperature within the laboratory was controlled between 46-67% and 21-24°C, respectively.

The following baseline measurements were used for two purposes within this paper. First, baseline measurements for 115, 117 and 1110 samples establishes how the raw data compares between the different material thicknesses. Second, establishing baseline measurement values, for each characterization technique before experimentation, is necessary to gauge the magnitude of degradation for each sample.

4.2. Energy Dispersive Spectroscopy (EDS) Measurements

Energy Dispersive Spectroscopy (EDS) baseline measurements were performed on the 115, 117 and 1110 samples to establish elemental composition consistency between each material.

Figure 6 shows raw EDS scans from untested dry 115 (yellow line), 117 (orange line) and 1110 (red line) samples. All three scans are nearly identical which indicates that the samples have similar elemental compositions. In addition, the primary elements in all three samples was carbon (C), oxygen (O), fluorine (F) and sulfur (S). The gold (Au) was from gold sputter-coated onto the sample surface to increase the electrical conductivity and trace potassium (K) was from handling the samples during the SEM mounting process. This elemental composition matches elements previously reported in literature [11, 12] for Nafion©. Fluorine had the largest peak, which seems reasonable, since the repeat unit for Nafion© is primarily composed of fluorine atoms. The approximate percentage of each atom in the Nafion© repeat unit taken from literature [11] is: 51.5% F, 27.3% C, 15.2% O, 3.0% S and 3.0% H. The ratios between these elements reported in literature do not exactly match the raw data collected in Figure 6, which is possibly due to a slightly different repeat unit structure used in literature. Overall, fluorine was still the largest elemental contributor and no additional elements are found compared to the EDS results in this paper.

4.3. Thermal Gravimetric Analysis (TGA) Measurements

Thermal Gravimetric Analysis (TGA) baseline measurements were performed on the 115, 117 and 1110 samples to establish each material had similar decomposition events and that decomposition temperatures were also similar. Differences in thermal degradation behavior between untested samples could influence results at elevated experimental temperatures (such as 120°C or 140°C) and needs to be accounted for.

Figure 6: Raw EDS Baseline Measurements of Untested Dry 115, 117 and 1110 Samples

Figure 7 shows the raw TGA data from untested dry 115 (blue line), 117 (green line) and 1110 (orange line) samples. All three materials have nearly identical thermal decomposition profiles between 21°C and 700°C, which indicates the material thickness did not have any impact on the thermal degradation profile. All three materials remained thermally stable (did not have a decomposition event) until ~300°C where the primary decomposition event occurred. Any mass loss between 21°C and 300°C was attributed to water loss within each sample, not from sample decomposition. These results also demonstrate that the temperatures used in this study will not result in thermal decomposition of the samples. Changes in dry sample mass before and after experimentation are a secondary method to validate decomposition did not occur.

4.4. Scanning Electron Spectroscopy (SEM) Measurements

Scanning Electron Microscopy (SEM) micrographs of untested dry 115, 117 and 1110 samples were taken to determine whether differences in the sample surfaces were present. Surface defects, such as holes, could contribute to material failure or other deviations in other properties.

Figure 8 shows the SEM micrographs of untested dry 115 (top), 117 (middle) and 1110 (bottom) samples. All three samples appear to be defect-free while the smaller particles on the surface were nano-sized or micron-sized dust particulates. Some slight surface topography irregularities were observed, but those are not expected to impact the material properties. Overall, all three sample materials micrographs appear to be identical.

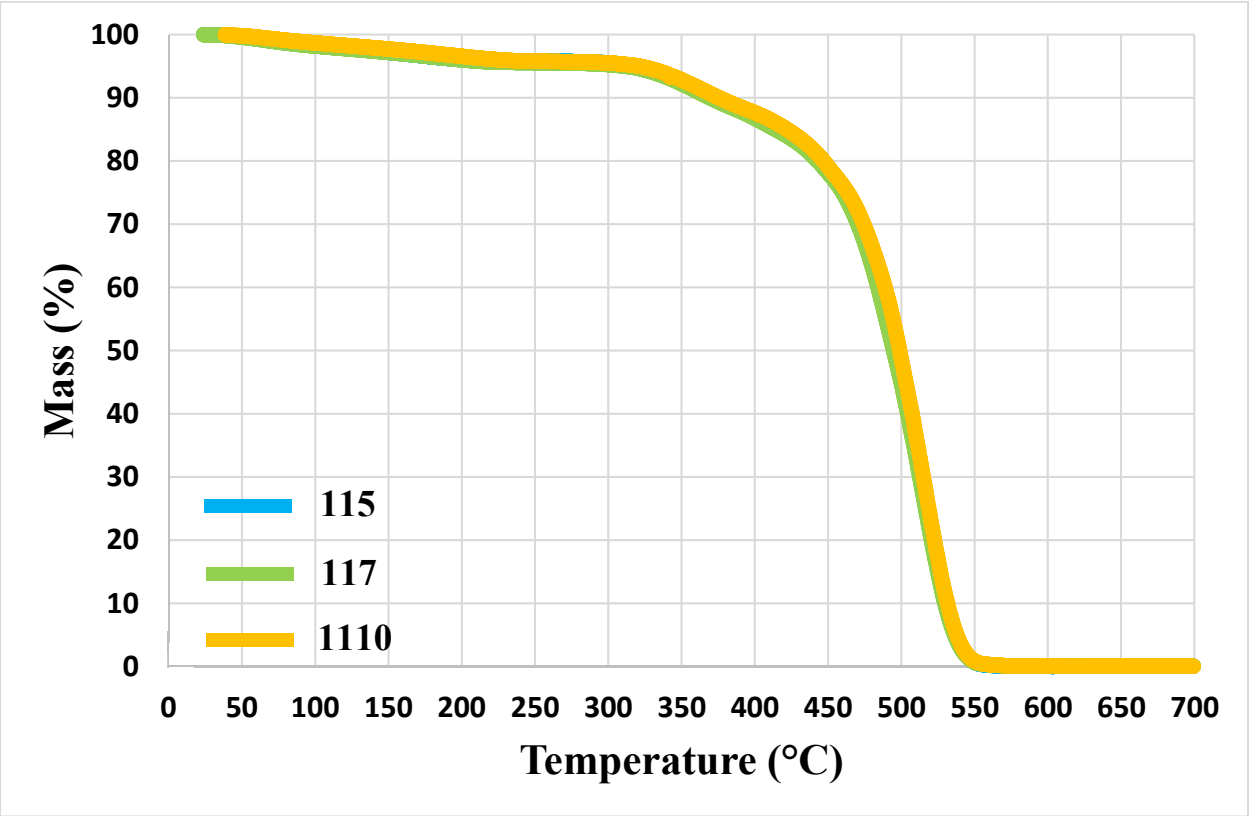

Figure 7: Raw TGA Baseline Measurements of Untested Dry 115, 117 and 1110 Samples

4.1. Electrochemical Impedance Spectroscopy (EIS) Measurements

Electrochemical Impedance Spectroscopy (EIS) measurements were performed on the 115, 117 and 1110 samples to establish the impact material thickness had on proton conductivity through the material and to establish a baseline for future experiments. As mentioned in Section 3 there are two variables, ohmic resistance and sample thickness, which can impact the conductivity values and need to be determined.

Table 1 shows the untested saturated 115, 117 and 1110 calculated and measured conductivity parameters, which are graphically depicted in Figure 10, Figure 11 and Figure 12 below for easier comparison.

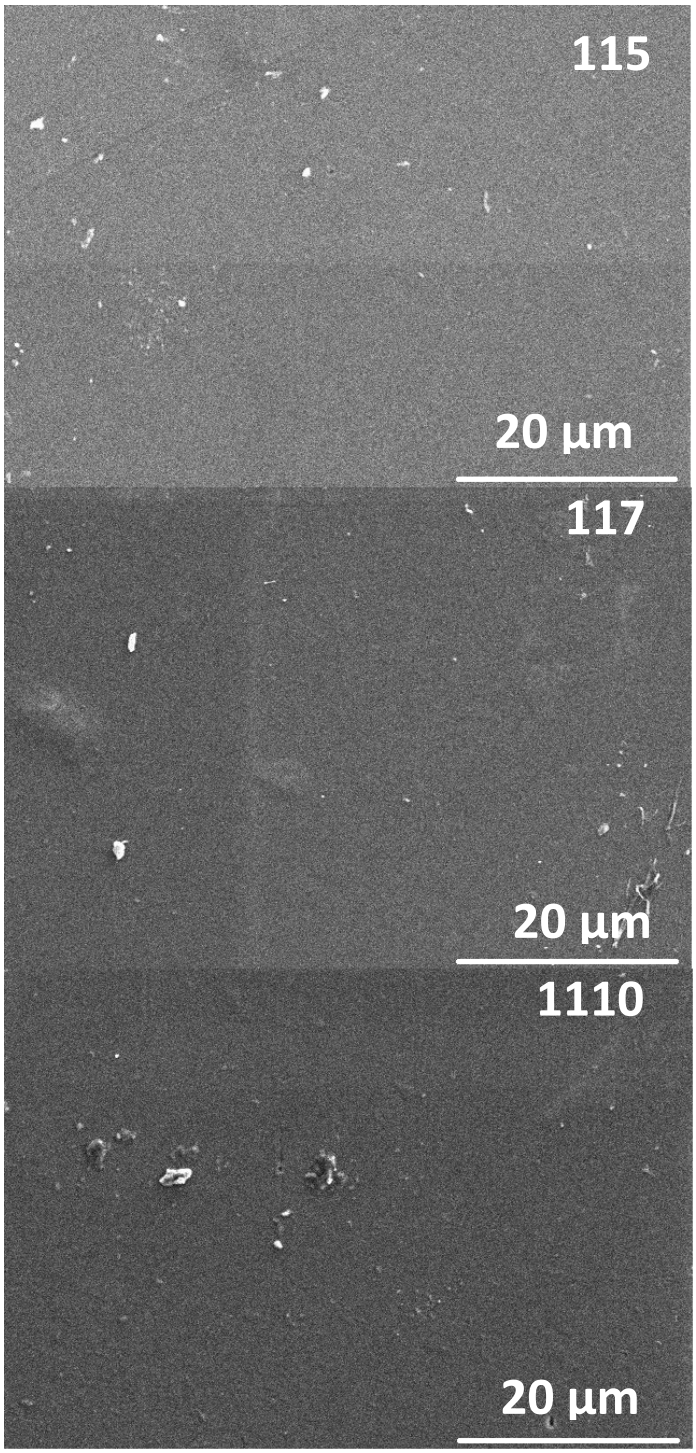

Figure 8: SEM Baseline Micrographs of Untested Dry 115, 117 and 1110 Samples

Table 1: Average EIS Baseline Untested Saturated 115, 117 and 1110 Sample Calculated and Measured Conductivity Parameters

Material Type	Average Proton Conductivity (S/cm)	Average Ohmic Resistance (Ω)	Average Sample Thickness (µm)	Average Proton Conductivity SD	Average Ohmic Resistance SD
115	0.02242	3967	127.0	0.0014	251.7
117	0.02078	2680	203.2	0.0017	213.8
1110	0.02332	1737	279.4	0.0019	148.0

Figure 9 shows the raw EIS data from the untested saturated 115 (blue diamonds), 117 (green squares) and 1110 (orange triangles) samples. The data shown in Figure 9 is a representation of the average values obtained from all the tested samples for each material. Overall, the resistance values (difference between the origin and data intercept with x-axis) decrease as the material thickness increases. This is possibly due to an increased water content as the material thickness increases.

Figure 10 shows the average calculated proton conductivities (using equations 2 and 3) for untested saturated 115 (blue bar, left), 117 (green bar, center) and 1110 (orange bar, right) samples. Calculated conductivity values used results from Figure 9 and Table 1. Overall, the calculated conductivity values for the three samples are statistically similar and their average values are only marginally different. Even though the conductivity values are similar the calculated ohmic resistances and measured sample thicknesses could be different and will be examined.

Figure 11 shows the average measured sample thicknesses for untested saturated 115 (blue bar, left), 117 (green bar, center) and 1110 (orange bar, right) samples. Average saturated sample thickness values increased, in a near linear manner, as the untested dry sample thickness increased. Since the calculated conductivity values were very similar, and the measured material thickness values increased linearly, the ohmic resistance values are projected to decrease.

Figure 12 shows the average calculated ohmic resistances for untested saturated 115 (blue bar, left), 117 (green bar, center) and 1110 (orange bar, right) samples. Ohmic resistance values decreased, as predicted, as the initial sample thickness increased. As stated earlier, the decrease in ohmic resistance is hypothesized to be the result of an increase in water content as the material thickness increases. The sample length and width were held constant but sample thickness increased, so the total amount of water would increase as well. An increase in water would allow for more ions/electrons to flow and thus promote a lower ohmic resistance.

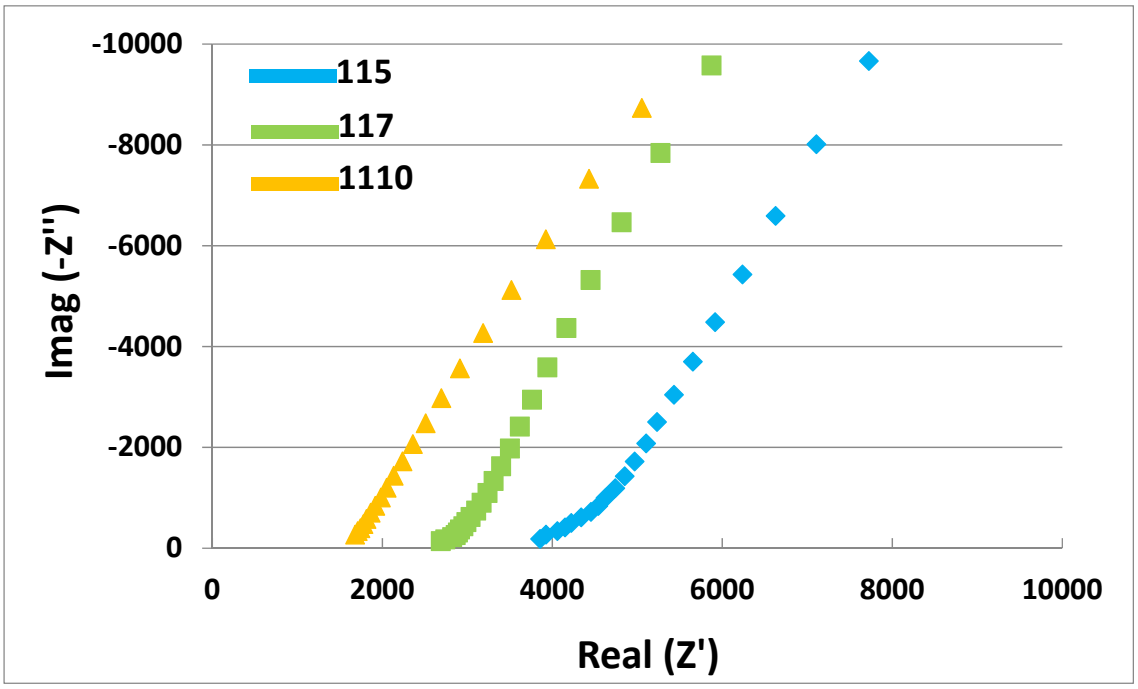

Figure 9: Raw EIS Baseline Scans of Untested Saturated 115, 117 and 1110 Samples

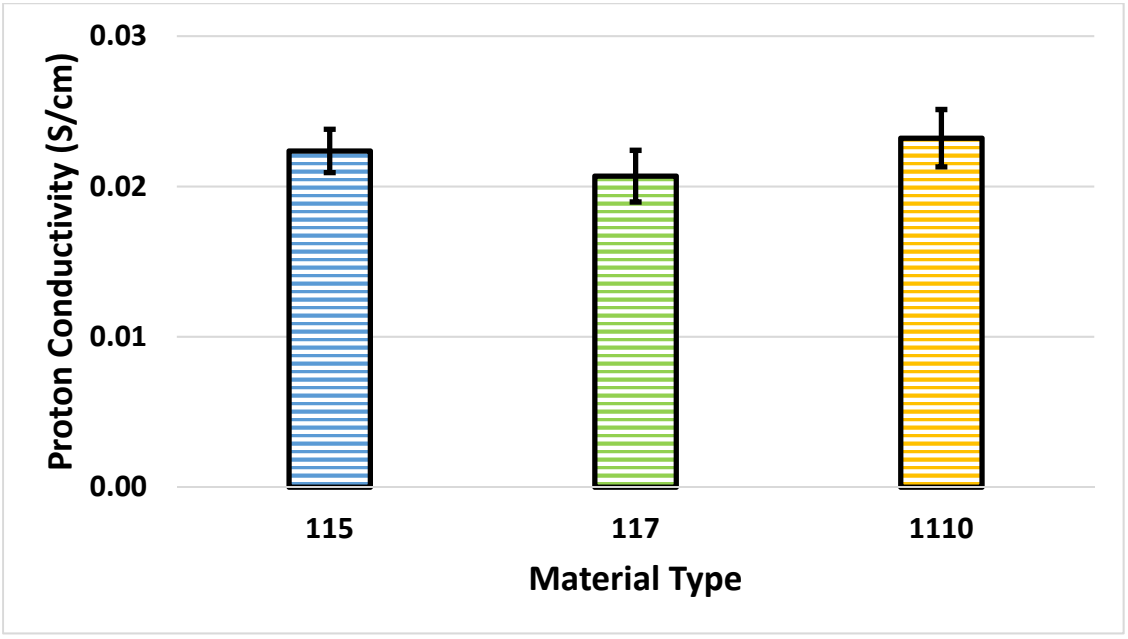

Figure 10: Average Calculated Baseline Proton Conductivity Data of Untested Saturated 115, 117 and 1110 Samples

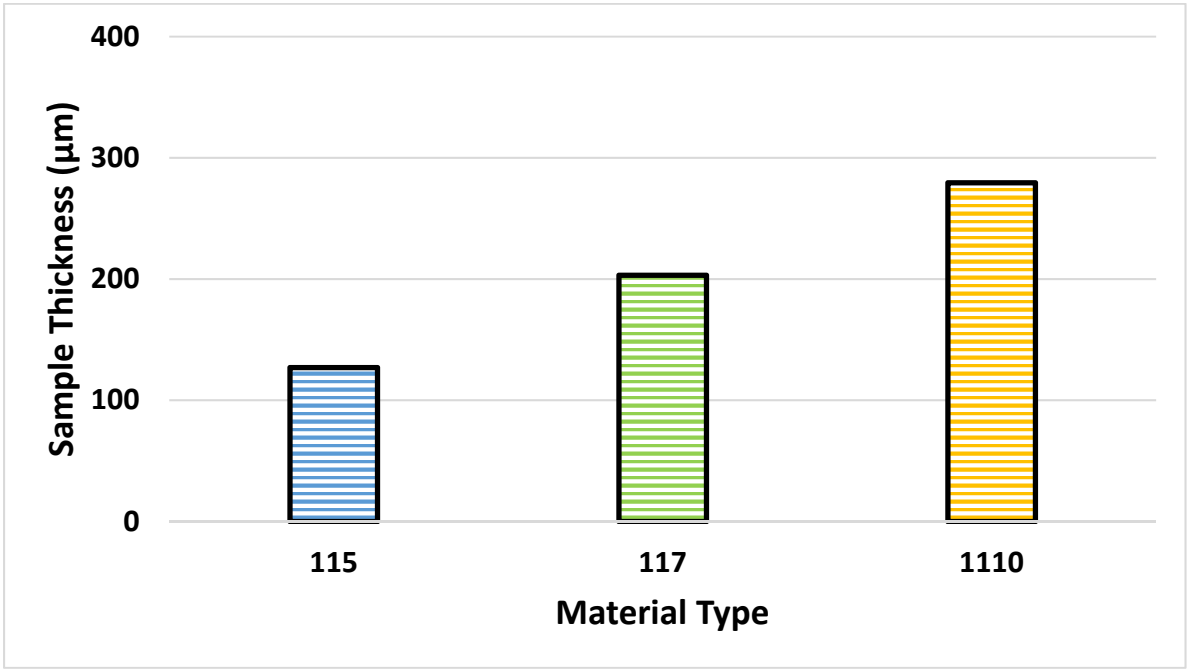

Figure 11: Average Measured Baseline EIS Thicknesses of Untested Saturated 115, 117 and 1110 Samples

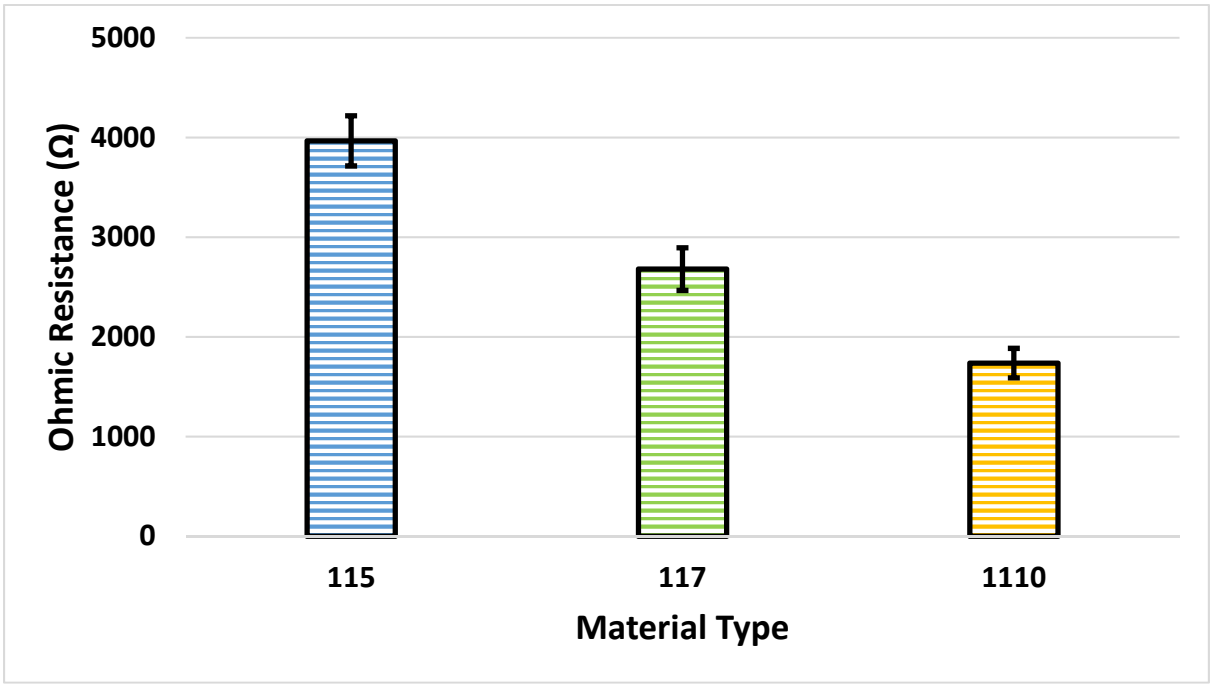

Figure 12: Average Calculated Baseline Ohmic Resistance Data of Untested Saturated 115, 117 and 1110 Samples

4.2. Mass Change Measurements

Mass change measurements were performed on each sample to determine if heating, cooling or freezing for prolonged periods of time caused any of the different material thicknesses to thermally degrade. Since no experiments had been performed the baseline mass change was 0%.

4.3. Water Absorption Measurements

Water absorption measurements were performed on each sample to determine whether the amount of water incorporated into the different samples changed after heating, cooling or freezing as a function of material thickness. The water capacity of each sample is important as that can help explain performance changes in the polymer membrane. Changes in the amount water, as a function of time, is important to know as the software used to operate the fuel cell stack is assuming those values are constant and would potentially make it more difficult for the stack to operate efficiently.

Table 2 shows the untested 115, 117 and 1110 measured dry and saturated mass values and the calculated water absorption percentage.

Table 2: Water Absorption Baseline Untested 115, 117 and 1110 Sample Parameters

Material Type	Average Dry Sample Mass (g)	Average Saturated Sample Mass (g)	Average Water Absorption (%)	Average Water Absorption SD
115	0.0432	0.0511	18.4	2.1
117	0.0531	0.0629	18.6	1.5
1110	0.0687	0.0825	20.1	0.1

Figure 13 shows the calculated water absorption percentages for untested saturated 115 (blue bar, left), 117 (green bar, center) and 1110 (orange bar, right) samples. Saturating each sample for 1 hour in 16MΩ water increased their average mass to 18.4-20.1% while all three values were within their standard deviation.

4.4. Fourier-Transform Infrared (FTIR) Spectroscopy Measurements

Fourier-Transform Infrared (FTIR) spectroscopy measurements were performed on the 115, 117 and 1110 samples to determine whether different vibrational modes were present after degradation based on the starting sample thickness. Differences in the vibrational modes can lead to differences in performance values. Even though all three materials have shown no statistical changes in proton conductivity there still may be differences in the internal behavior between each material that could result in other mechanical property differences.

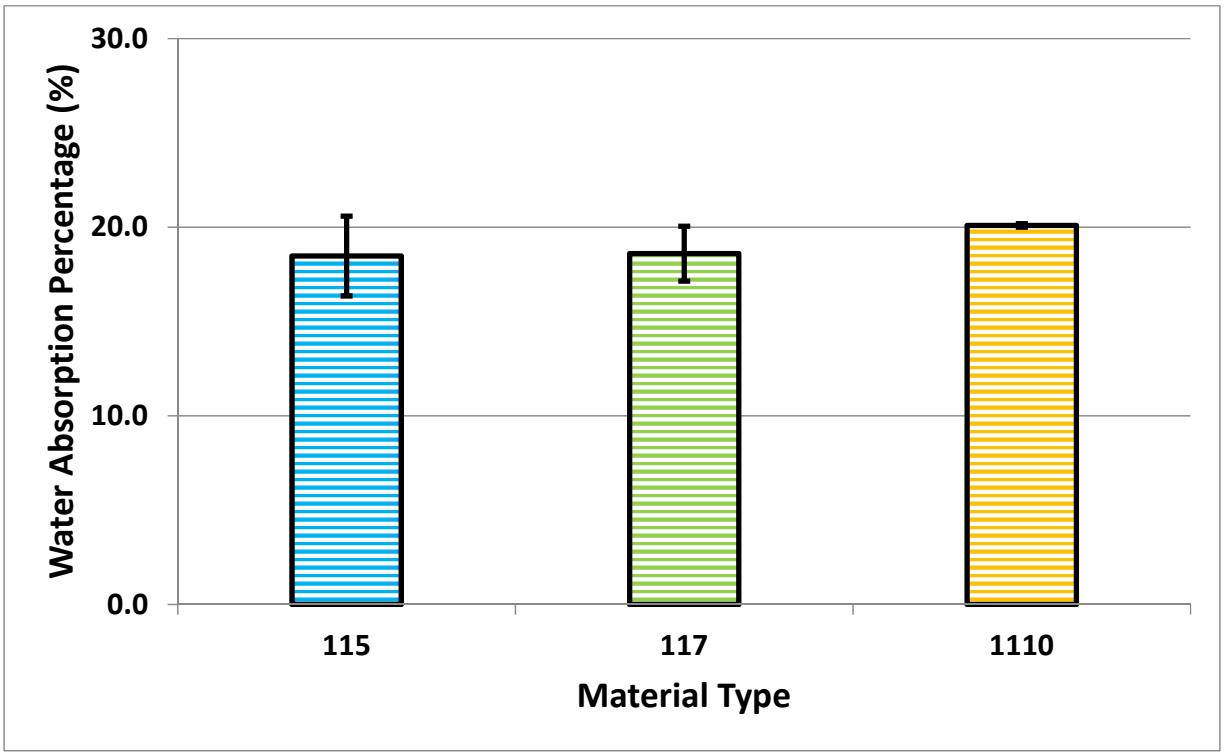

Figure 13: Calculated Baseline Water Absorption % of Untested Saturated 115, 117 and 1110 Samples

Figure 14 shows the raw FTIR scans for untested dry 115 (blue data), 117 (green data) and 1110 (orange data) samples. Inspection of the raw data indicates all three datasets are nearly identical, at least when the data is viewed using this expanded view. In addition the modes from the Nafion© material itself (opposed to water within each sample) starts around wavenumber 1,500 cm^{-1}, which also matches other literature studies [13, 14, 15] which show vibrational modes in Nafion© samples between 4,000 cm^{-1} and 1,500 cm^{-1} are from water within the sample. Finally, despite the three samples appearing nearly identical, small details in peak shape may be present. The following figure will take a closer look between 1,500 cm^{-1} and 500 cm^{-1} wavenumbers to determine if each sample is identical.

Figure 15 shows the same raw FTIR data from Figure 14 but focuses on the data between 1,500 cm^{-1} and 675 cm^{-1} wavenumbers so finer details of each peak can be inspected. Overall each sample appears to be nearly identical. There may be slight differences in slope (which is hypothesized to be the result of small differences in sample fabrication) there does not appear to be any differences worth mentioning. The following peaks and possible vibrational modes have been identified from literature, which are listed in Table 3 below. The peak of each vibrational mode for the collected data may be a few wavenumbers different from the reported values in the literature studies, which is acceptable. The small differences can be attributed to small differences in the materials used or small differences in the equipment used between each study.

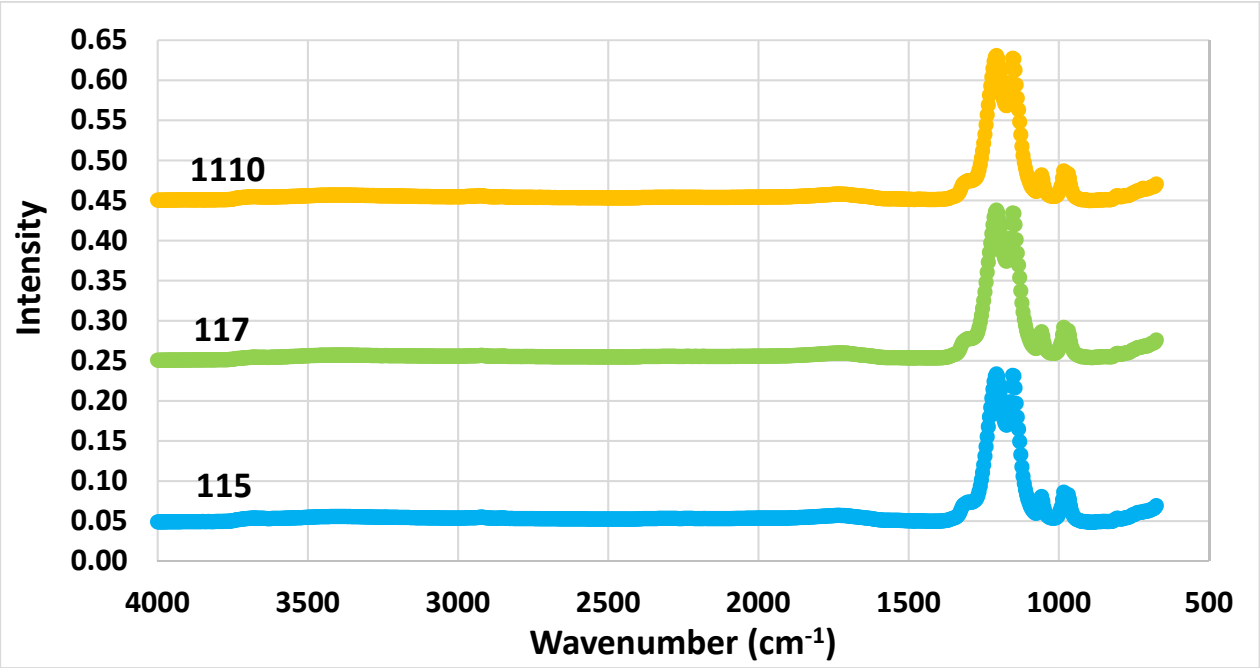

Figure 14: Raw FTIR Baseline Scans of Untested Dry 115, 117 and 1110 Samples 4000 cm^{-1} to 675 cm^{-1}

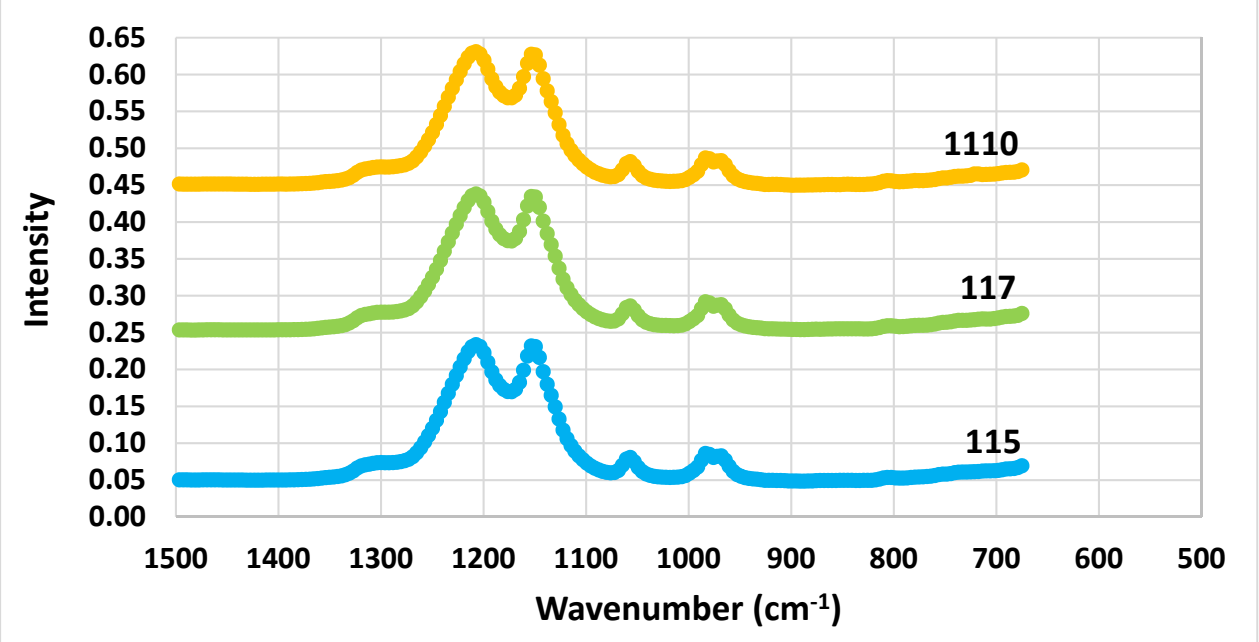

Figure 15: Raw FTIR Baseline Scans of Untested Dry 115, 117 and 1110 Samples from 1500 cm^{-1} to 675 cm^{-1}

Table 3: Vibrational Mode Peak Assignments for Untested Dry 115, 117 and 1110 Samples

Wavenumber (cm^{-1})	Literature Wavenumber Band Assignment	Vibrational Mode Band Assignments	Literature References
1307	1299	v[CC]	[16, 17, 18]
1203	1196 1212	v_a[CF_2] v_{as}[CF_2]	[16, 17, 18]
1149	1148 1148	v_s[CF_2] δ[FCF]	[16, 17, 18]
1060	1056	v_s[.SO_3^-]	[14, 19, 20]
979	983	v_{as}[C-O-C]	[14, 19, 20]
968	970	v_s[C-O-C]	[14, 19, 20]
806	805	v[CS]	[14, 16, 17, 18]

V = Stretching; V_{as} = Asti-symmetric Stretching' V_s = Symmetric Stretching; δ = Bending

4.5. X-Ray Diffraction (XRD) Measurements

X-Ray Diffraction (XRD) scans were performed on the 115, 117 and 1110 samples to determine whether the crystal structure, if present, was different as the sample thickness changed.

Figure 16 shows the raw XRD data for the untested dry 115 (blue data), 117 (green data) and 1110 (orange data) samples. A literature reference [21] is also included (black data) within the plot to provide supporting evidence the peaks shown in this paper are representative of Nafion© membranes. Overall, the raw data for all three samples was close to each other and had the same peak positions as the literature reference. Samples contained two peaks, located at ~17° and ~39.5° 2-Theta, which will be referred to as Peak I and Peak II, respectively, for the remainder of this paper. Both peaks were semi-crystalline and the only difference between these scans was the 115 and 1110 Peak I intensities were higher than the 117 Peak I intensity. Differences in individual peak intensity values is not an adequate method of comparison between different materials and the ratio between the different peaks intensities (within a single scan) need to be compared instead to determine if an actual difference exists.

Figure 17 shows the calculated peak intensity ratios between the Peak I and Peak II for the untested dry 115 (blue data), 117 (green data) and 1110 (orange data) samples. There does appear to be small differences in the calculated peak intensity ratios but there does not appear to be a trend to the results and differences are still within the calculated standard deviation, so are not statistically significant.

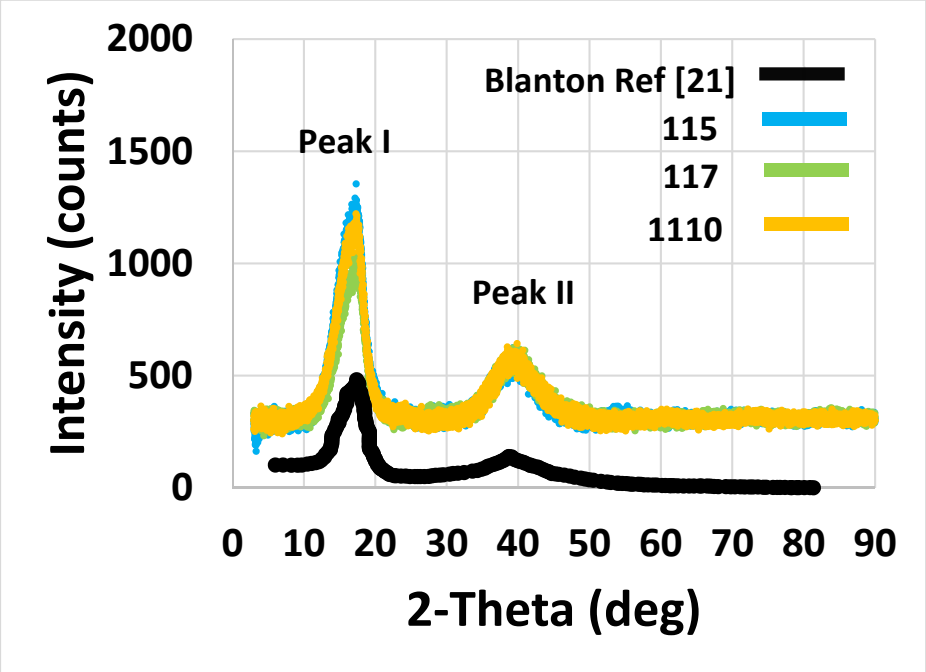

Figure 16: Raw XRD Baseline Scans of Untested Dry 115, 117 and 1110 Samples. Reference from literature [21] shown in black.

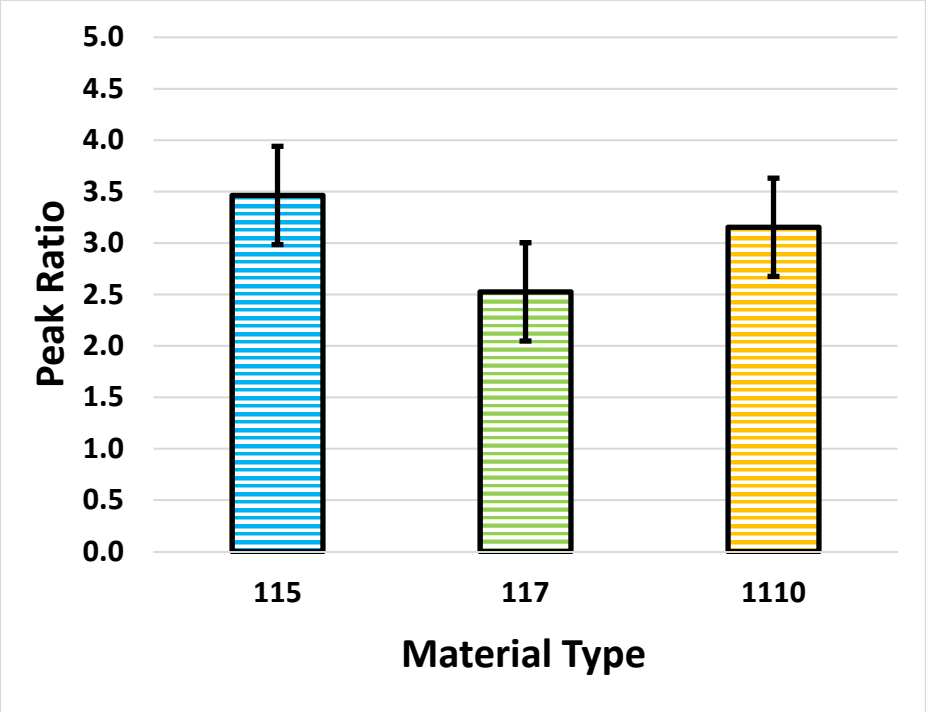

Figure 17: Calculated XRD Baseline Scan Peak Intensity Ratios of Untested Dry 115, 117 and 1110 Samples

4.6. Baseline Material Characterization Summary

The characterization measurements in this section verified all the sampled used in this study were Nafion©. These characterization tests also showed that the 115, 117 and 1110 samples had nearly identical baseline behavior for TGA thermal decomposition, SEM micrographs, mass change, water absorption percentage, FTIR vibrational modes and XRD scans.

The following section will investigate the effect of heating at 65°C, 120°C and 140°C for 2, 8 and 24 hours, in a 5 vol% acetic acid solution, to see if prolonged exposure to a slightly acidic solution at elevated temperatures impacts the characterization data for any material thickness. These results will also be contrasted to previous data collected that investigated proton conductivity changes in Nafion© 115, 117 and 1110 samples only exposed to elevated temperatures.

5. Proton Conductivity Comparison Between Heated Samples with and without 5 vol% Acetic Acid

5.1. Introduction

This section will characterize the proton conductivity of the 115, 117 and 1110 samples using EIS. Raw EIS data from samples, heated to 65°C, 120°C and 140°C for 2, 8 and 24 hours in 5 vol% acetic acid, will be used to calculate sample proton conductivity using Equation 1 and 2 shown in Section 3. These results will be contrasted against results from: 1. Samples previously heated at the same temperatures in solutions containing only 16 MΩ water and 2. Baseline measurements taken at 21°C.

Manufacturers typically recommend PEMFC stacks not to exceed an operating temperature of 65°C, which is why 65°C was used as the minimum heating temperature. Testing at 65°C for different periods of time provided an operational baseline to compare against the untested baseline measurements and the future tests at 120°C and 140°C for prolonged periods of time.

5.2. Proton Conductivity Characterization at 21°C

Proton conductivity degradation will first be compared at 21°C using acetic acid and then to samples saturated in 16 MΩ water. As mentioned, results in this section will establish a baseline of how sensitive each sample is to acetic acid without the effects of heat introduced.

Figure 18 shows the calculated average ohmic resistance data for the saturated 115 (blue bars), 117 (green bars) and 1110 (orange bars) samples heated to 21°C. Over the 24 hour testing period ohmic resistance values of the each sample stayed relatively constant but were lowered slightly compared to their untested baseline counterpart. All samples were statistically lower than their respective untested baseline, expect for the 115 sample, which only became statistically similar at the 24 hour mark and was outside the standard deviation for all other measurements. Ohmic resistance values were found to be lowered between 10-32% from their untested baselines.

Figure 19 shows the average measured sample thicknesses for the saturated 115 (blue bars), 117 (green bars) and 1110 (orange bars) samples heated to 21°C. Sample thickness values did not change, after being heated to 21°C, when compared to their untested baseline values over the 24 hour period.

Figure 20 shows the average calculated proton conductivity values for the saturated 115 (blue bars), 117 (green bars) and 1110 (orange bars) samples heated to 21°C. Results that used acetic acid were shown as bars with no black outline and results that did not use acetic acid were shown as bars with a solid black outline. Since the ohmic resistance, shown in Figure 18, was reduced and the sample thickness did not change, it is not surprising the proton conductivity for all samples exposed to acetic acid was increased compared to the baseline. These values are also statistically larger than the calculated proton conductivities with no acetic acid, which indicates acetic acid, even near room temperature, has a noticeable effect on the material properties of Nafion©.

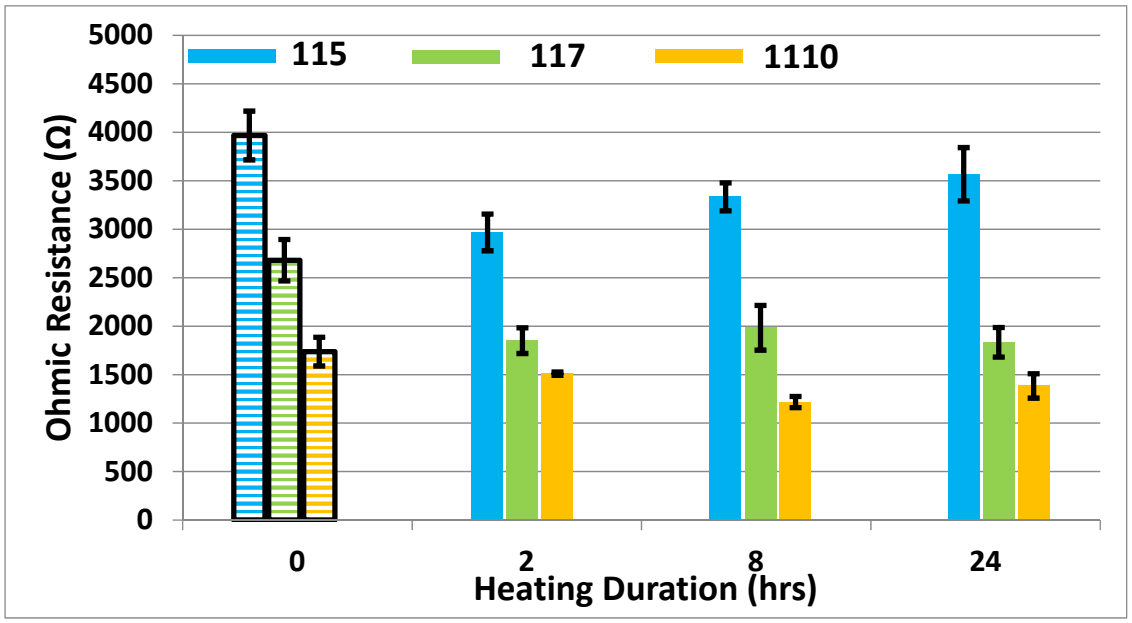

Figure 18: Average Calculated Ohmic Resistance Data of Saturated 115, 117 and 1110 Heated to 21°C for 2, 8 and 24 hours. Samples Heated in 5 vol% Acetic Acid are Shown as Solid Bars with no Outline. Baseline Results are Shown as Open Bars with Horizontal Lines.

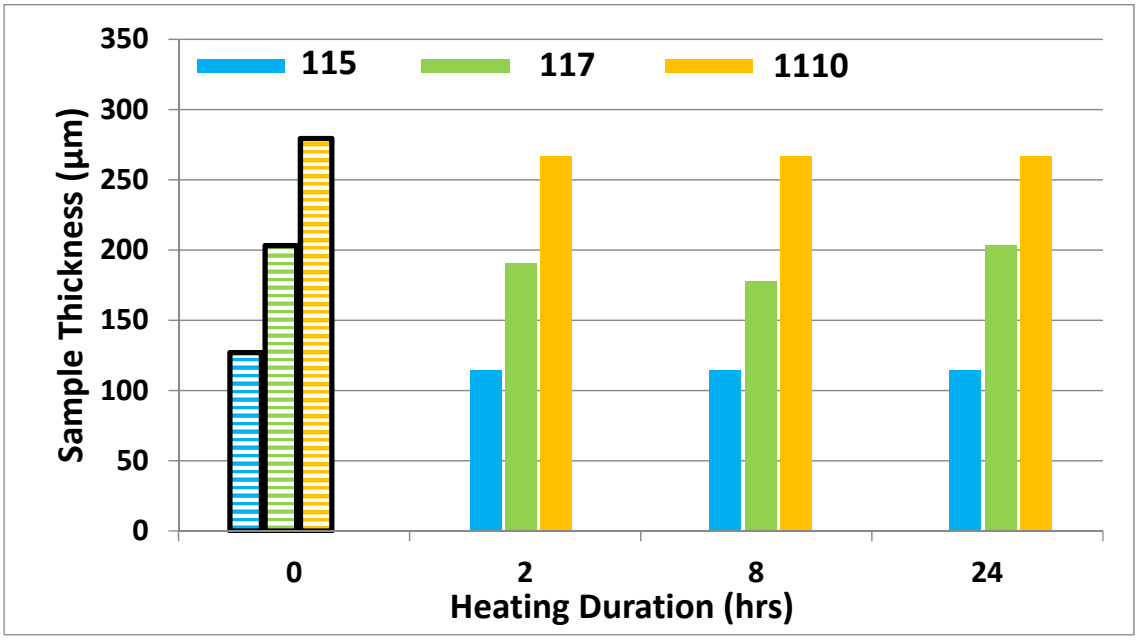

Figure 19: Average Measured Sample Thicknesses of Saturated 115, 117 and 1110 Heated to 21°C for 2, 8 and 24 hours. Samples Heated in 5 vol% Acetic Acid are Shown as Solid Bars with no Outline. Baseline Results are Shown as Open Bars with Horizontal Lines.

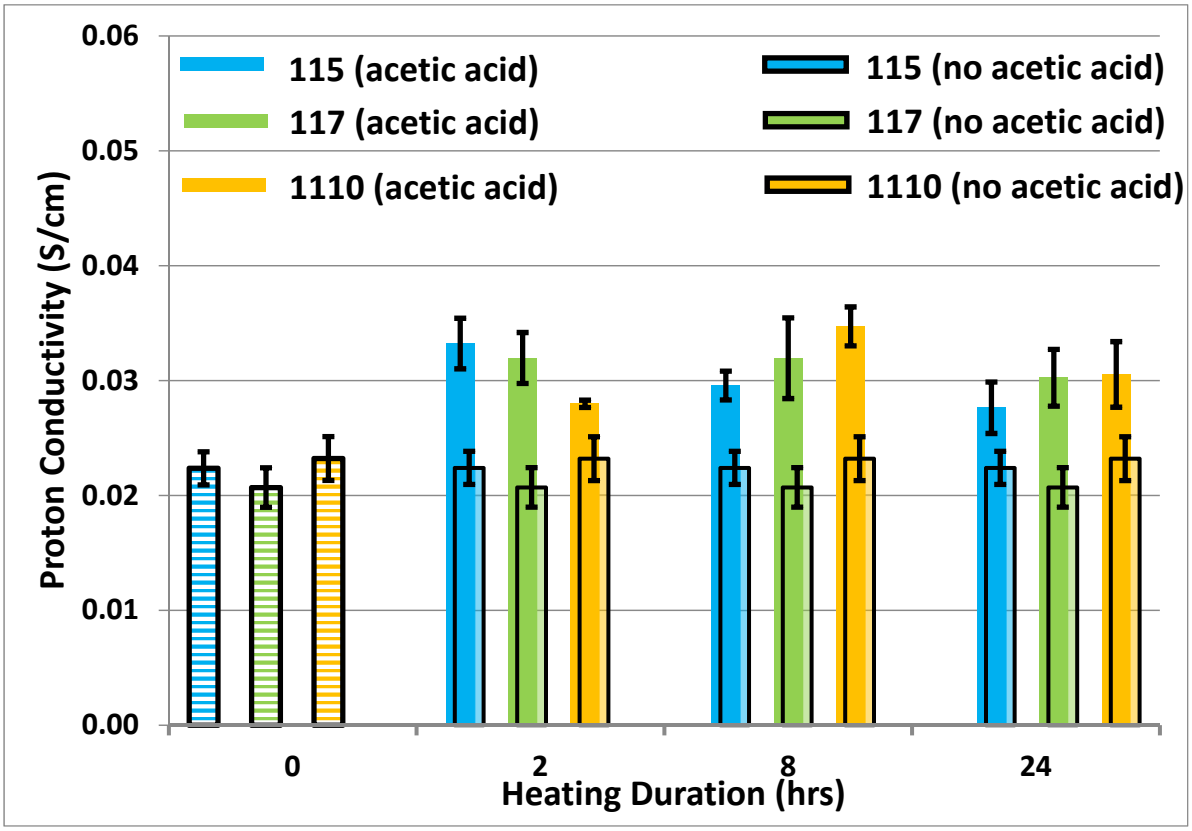

Figure 20: Average Calculated Proton Conductivity for Saturated 115, 117 and 1110 Heated to 21°C for 2, 8 and 24 hours. Samples Heated in 5 vol% Acetic Acid are Shown as Solid Bars with no Outline. Samples Heated in Water are Shown as Open Bars with Black Outlines. Baseline Results are Shown as Open Bars with Horizontal Lines.

5.3. Proton Conductivity Characterization at 65°C

Proton conductivity degradation will first be investigated at 65°C using acetic acid and then compared to samples saturated in 16 MΩ water. This temperature is close to where many PEM fuel manufacturers recommend operating the stack. Results presented in this section will be a decent overall guide to determine if low concentrations of acetic acid would have detrimental effects on the proton conductivity performance of the PEM fuel cell membrane.

Figure 21 shows the calculated average ohmic resistance data for the saturated 115 (blue bars), 117 (green bars) and 1110 (orange bars) samples heated to 65°C. Ohmic resistance decreased initially after 2 hours of exposure to acetic acid, but then started to gradually increase, except for the 115 sample which became extremely resistive after 24 hours. This drastic change in ohmic resistance for 115 may indicate significant structural degradation to the point where protons cannot be transported efficiently. The 115 is the thinnest material so observing it degrade first is not surprising. These results also show that even at traditional stack operating temperatures the presence of low concentrations of acetic acid can have dramatic impacts on membrane properties.

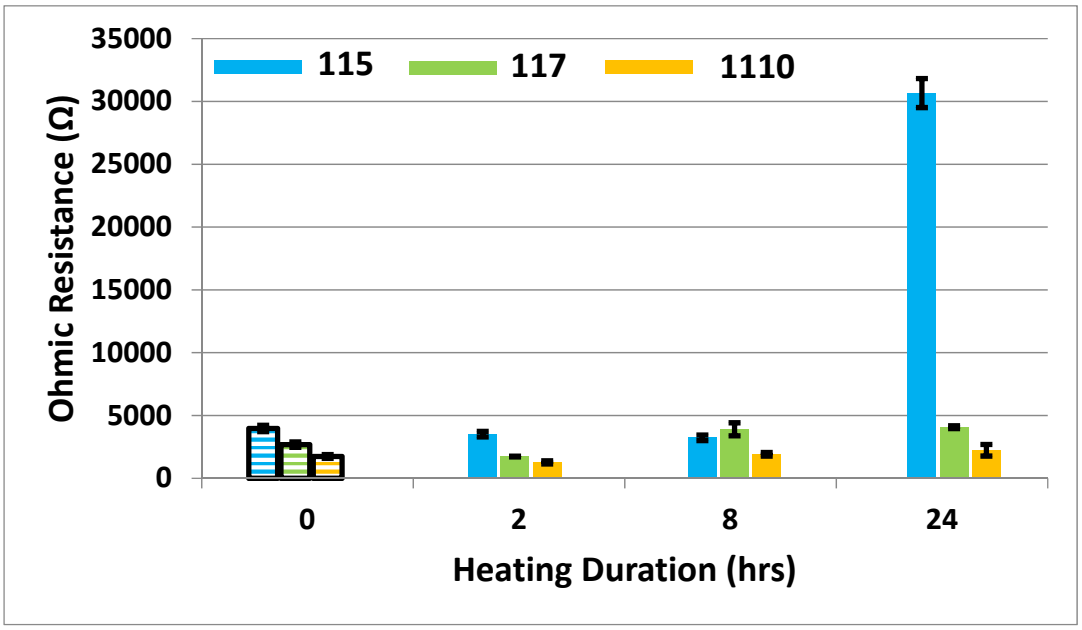

Figure 21: Average Calculated Ohmic Resistance Data of Saturated 115, 117 and 1110 Heated to 65°C for 2, 8 and 24 hours. Samples Heated in 5 vol% Acetic Acid are Shown as Solid Bars with no Outline. Baseline Results are Shown as Open Bars with Horizontal Lines.

Figure 22 shows the average measured sample thicknesses for the saturated 115 (blue bars), 117 (green bars) and 1110 (orange bars) samples heated to 65°C. Samples stayed relatively constant in thickness compared to their baseline measurements.

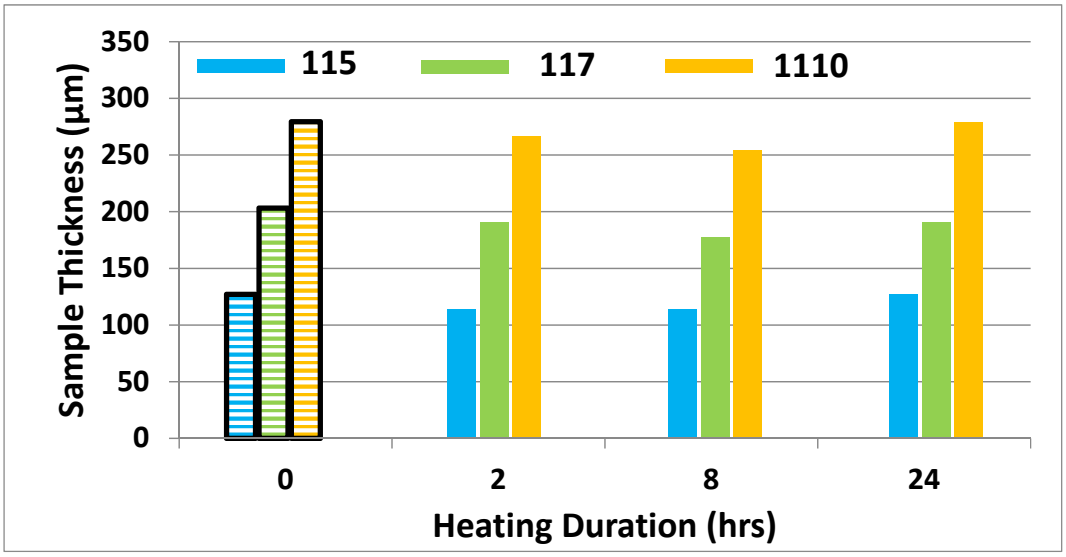

Figure 22: Average Measured Sample Thicknesses of Saturated 115, 117 and 1110 Heated to 65°C for 2, 8 and 24 hours. Samples Heated in 5 vol% Acetic Acid are Shown as Solid Bars with no Outline. Baseline Results are Shown as Open Bars with Horizontal Lines.

Figure 23 shows the average calculated proton conductivity values for the saturated 115 (blue bars), 117 (green bars) and 1110 (orange bars) samples heated to 65°C. Unlike the calculated proton conductivities for samples heated to 21°C, which were constantly greater than the baseline, the following results start to decrease their proton conductivity values. When compared to the acetic acid 21°C results these values are consistently lower after even heating duration. These results also show all three samples start to degrade performance even after 8 hours of heating, although the 115 sample was significantly greater. The larger decrease in conductivity of the 115 could be partly contributed to its observed change in ohmic resistance.

Finally, when compared to heating alone, heating in the presence of acetic acid lowered the proton conductivity even further. This can be observed after the samples were heated for at least 8 hours. Samples that were heated without acetic acid maintained an increased proton conductivity over the baseline around 25%. In contrast the samples heated using acetic acid reduced their conductivity, on average, to ~5% above the baseline after 8 hours and reduced their proton conductivities to 86% below the baseline, on average, after 24 hours of heating in the presence of acetic acid.

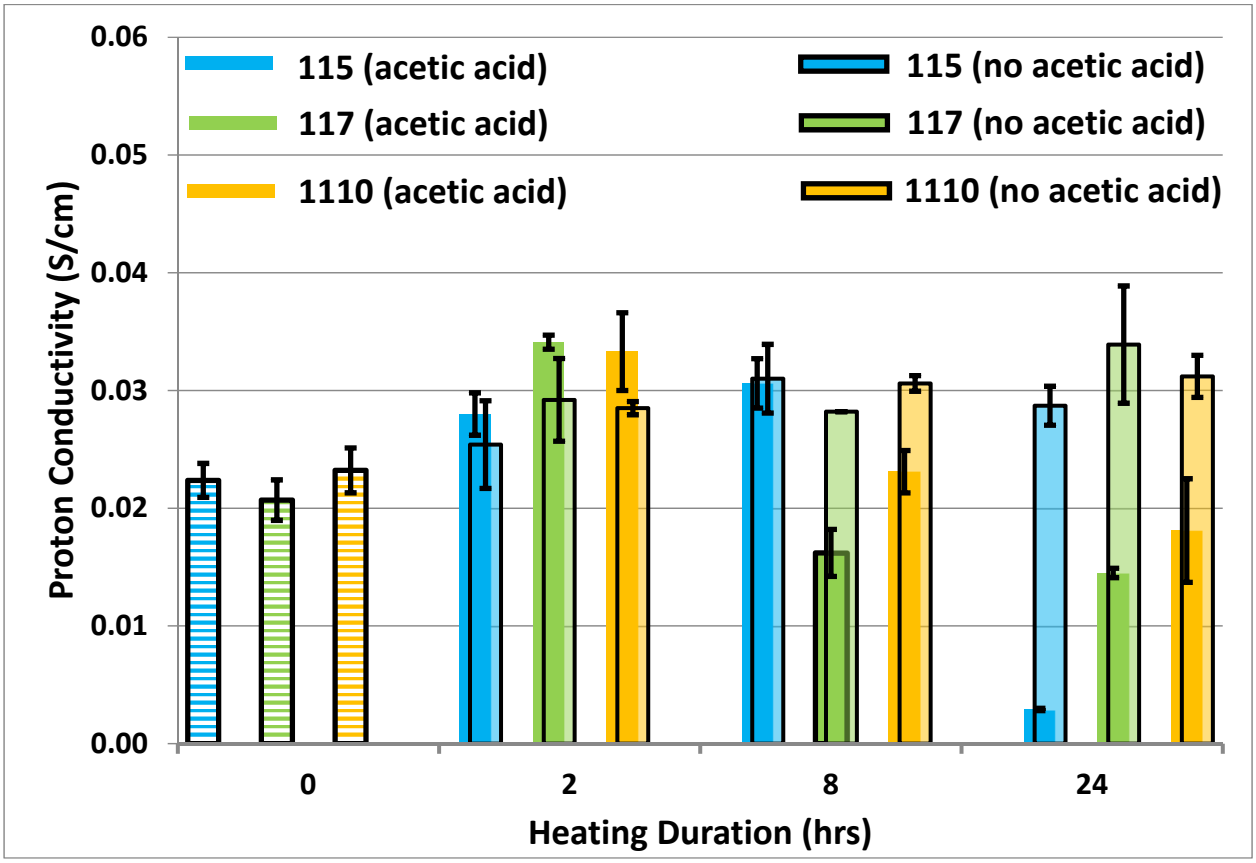

Figure 23: Average Calculated Proton Conductivity for Saturated 115, 117 and 1110 Heated to 65°C for 2, 8 and 24 hours. Samples Heated in 5 vol% Acetic Acid are Show as Solid Bars with no Outline. Samples Heated in Water are Shown as Open Bars with Black Outlines. Baseline Results are Shown as Open Bars with Horizontal Lines.

5.4. Proton Conductivity Characterization at 120°C

This section investigates temperatures above 100°C starting at 120°C, which is significantly greater than the recommended operating temperature.

Figure 24 shows the calculated average ohmic resistance data for the saturated 115 (blue bars), 117 (green bars) and 1110 (orange bars) samples heated to 120°C. The samples show some reduction in their resistance up to the 8 hour mark (compared to the baseline), but then increase after 24 hours as was seen with the samples heated to 65°C. Again the 115 increased the most of the three samples, which is hypothesized to be from the thinner sample thickness.

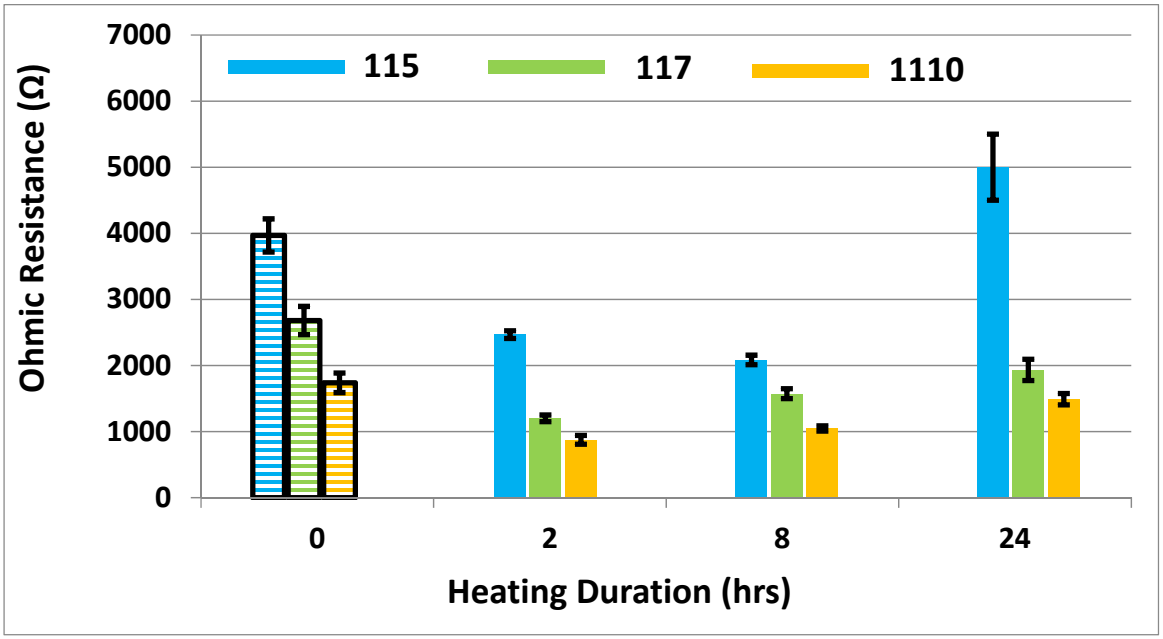

Figure 24: Average Calculated Ohmic Resistance Data of Saturated 115, 117 and 1110 Samples Heated to 120°C for 2, 8 and 24 hours. Samples Heated in 5 vol% Acetic Acid are Shown as Solid Bars with no Outline. Baseline Results are Shown as Open Bars with Horizontal Lines.

Figure 25 shows the average measured sample thicknesses for the saturated 115 (blue bars), 117 (green bars) and 1110 (orange bars) samples heated to 120°C. The increased operating temperature promoted the all samples to increase their thickness when saturated. Sample thickness did not change as a function of time.

Figure 26 shows the average calculated proton conductivity values for the saturated 115 (blue bars), 117 (green bars) and 1110 (orange bars) samples heated to 120°C. The increased temperature and 5 vol% acetic acid contributed to the increase degradation as a function of time. Proton conductivity values start to decrease around the 8 hour mark and drop off rapidly after 24 hours. While the acetic acid results are slightly higher here, after 24 hours, than the 65°C proton conductivities, they still decreased a similar magnitude. The 65°C conductivities were reduced, 2 hours to 24 hours, by 65% while these 120°C results were reduced by 45%.

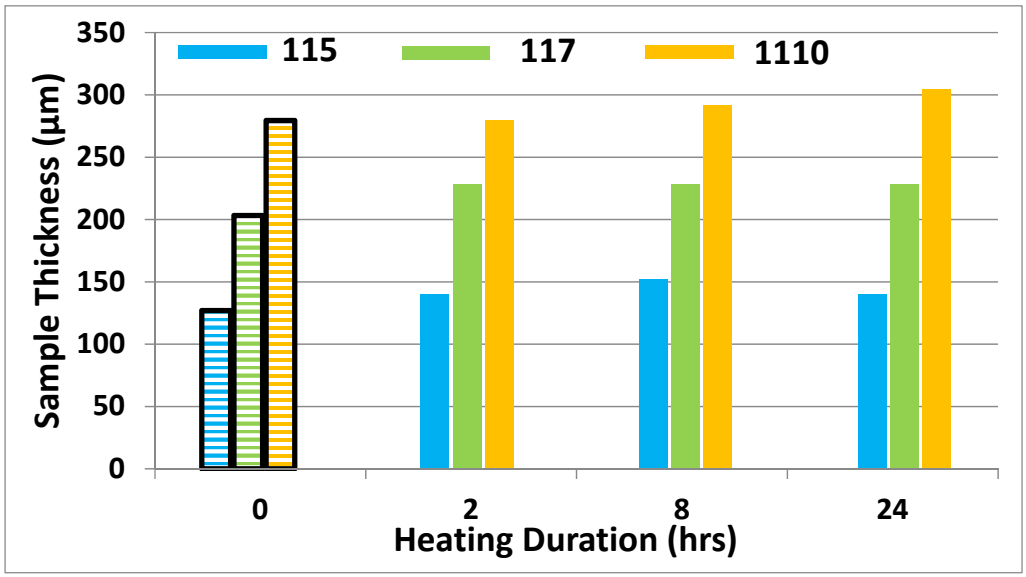

Figure 25: Average Measured EIS Characterized Sample Thicknesses of Saturated Nafion© 115, 117 and 1110 Heated to 120°C for 2, 8 and 24 hours. Samples Heated in 5 vol% Acetic Acid are Show as Solid Bars with no Outline. Baseline Results are Shown as Open Bars with Horizontal Lines.

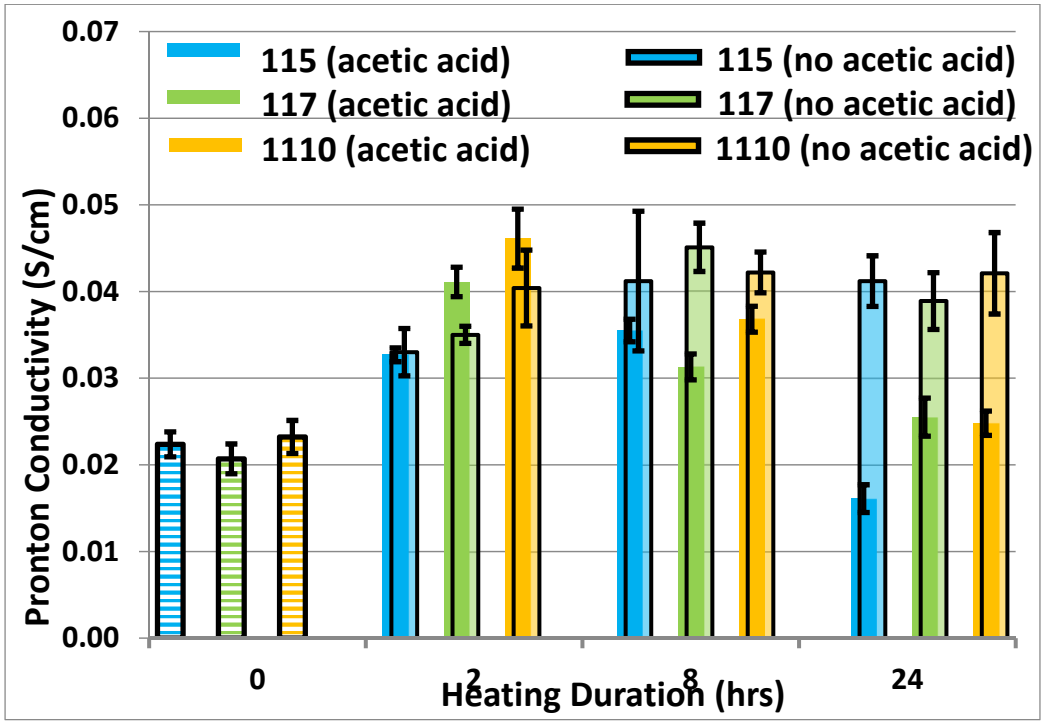

Figure 26: Average Calculated Conductivity for Saturated Nafion© 115, 117 and 1110 Heated to 120°C for 2, 8 and 24 hours. Samples Heated in 5 vol% Acetic Acid are Show as Solid Bars with no Outline. Samples Heated in Water are Shown as Open Bars with Black Outlines. Baseline Results are Shown as Open Bars with Horizontal Lines.

5.5. Proton Conductivity Characterization at 140°C

Figure 27 shows the calculated average ohmic resistance data for the saturated 115 (blue bars), 117 (green bars) and 1110 (orange bars) samples heated to 140°C. These result show a similar trend where the ohmic resistances are reduced after 2 hours, but the increased temperature now promotes increased resistance starting at 8 hours. In a similar manner, the 24 hour results show significant increases in resistance values for all three samples.

Figure 28 shows the average measured sample thicknesses for the saturated 115 (blue bars), 117 (green bars) and 1110 (orange bars) samples heated to 140°C. Just as was observed for the 120°C results the saturated sample thicknesses were increased, compared to the baseline, just to a larger extent.

Figure 29 shows the average calculated proton conductivity values for the saturated 115 (blue bars), 117 (green bars) and 1110 (orange bars) samples heated to 140°C. The results after heating are the most dramatic with proton conductivity values being reduced after only 2 hours compared to heating results using no acetic acid. The magnitude the proton conductivity increased, compared to the baseline, after 2 hours is also reduced compared to the previous heating results in this paper. After 24 hours all three samples show very little conductivity and are similar in their degradation. This illustrates that even the thickest (1110 sample), while being the most resilient up to now, is reduced to a similar state as the 115.

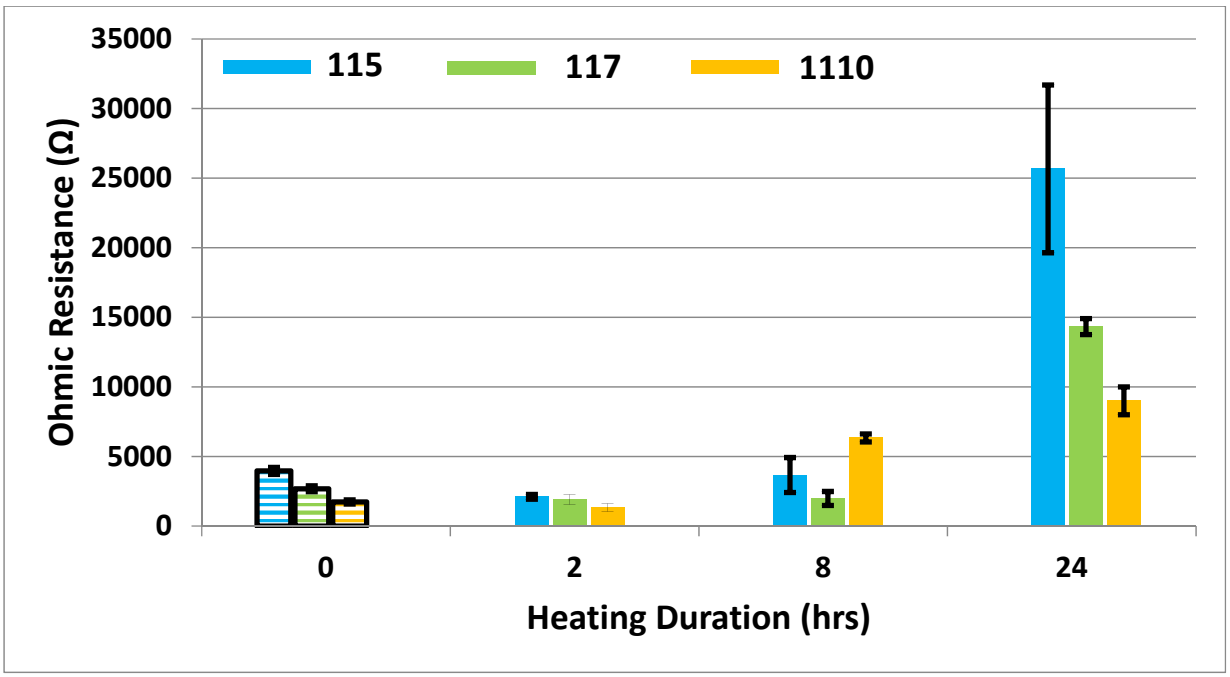

Figure 27: Average Calculated Ohmic Resistance Data of Saturated Nafion© 115, 117 and 1110 Heated to 140°C for 2, 8 and 24 hours. Samples Heated in 5 vol% Acetic Acid are Show as Solid Bars with no Outline. Baseline Results are Shown as Open Bars with Horizontal Lines.

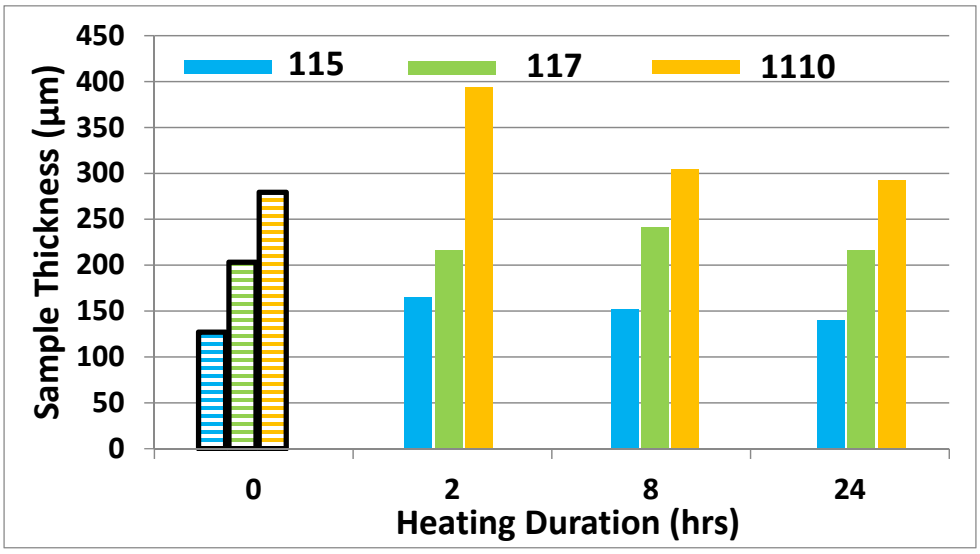

Figure 28: Average Measured EIS Characterized Sample Thicknesses of Saturated Nafion© 115, 117 and 1110 Heated to 140°C for 2, 8 and 24 hours. Samples Heated in 5 vol% Acetic Acid are Show as Solid Bars with no Outline. Baseline Results are Shown as Open Bars with Horizontal Lines.

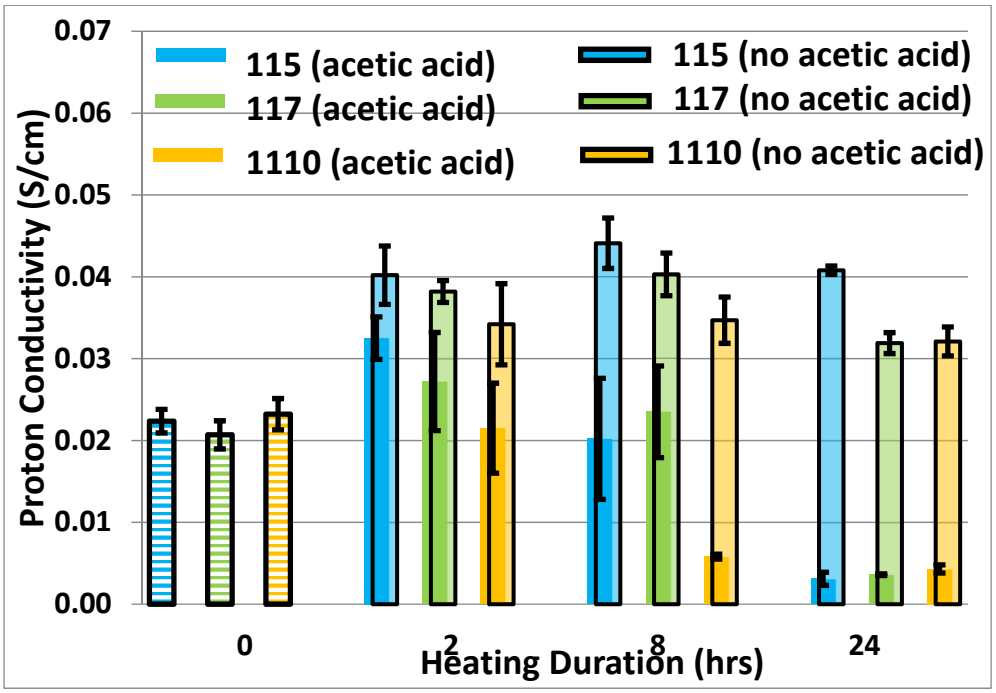

Figure 29: Average Calculated Conductivity for Saturated Nafion© 115, 117 and 1110 Heated to 140°C for 2, 8 and 24 hours. Samples Heated in 5 vol% Acetic Acid are Show as Solid Bars with no Outline. Samples Heated in Water are Shown as Open Bars with Black Outlines. Baseline Results are Shown as Open Bars with Horizontal Lines.

5.6. Proton Conductivity Measurement Summary and Conclusions

In summary, the following insights and conclusions can be taken away from the research presented in this paper, which hopefully will lead to improved PEM fuel cell designs with improved performance and increased durability.

First, the formation of acetic acid within the fuel cell had a significant impact on the ability of the electrolyte membrane to transport protons, even at low concentrations such as 5 vol%. As previously reported [6, 7] the formation of acetic acid inside the exhaust water can occur from the thermal degradation of the membrane itself. Thermal degradation alone dynamically increases the proton conductivity of the membrane over time, which cannot be ignored, but the addition of acetic acid also contributes to changes in proton conductivity beyond what heat alone demonstrated. As the results in the paper show, the proton conductivity is drastically decreased by the addition of acetic acid.

Second, the amount time required to observe changes in proton conductivity when acetic acid is present is very short at least in comparison to the expected multi-year operational life expectancy of PEM fuel cell stacks. Initial exposure to acetic acid at room temperature increased sample proton conductivity, while subsequent experiments using heat showed reductions in conductivity. Reductions in proton conductivity were observed within 8-24 hours of exposure to acetic acid while being heated when samples were heated at 65^{o}C and 120^{o}C, while heating at 140^{o}C decreased that time period to only 2 hours of exposure.

Third, changes in the sample proton conductivity can be described by changes in the ohmic resistance for proton transport within each sample and sample thickness. An increased ohmic resistance would result in reduced proton conductivity, while an increased sample thickness would increase the cross-sectional area of protons being transported through the material and also result in a lower proton conductivity (assuming a constant ohmic resistance). Primarily, changes in proton conductivity within samples heated at 21^{o}C and 65^{o}C were controlled only by statistically significant changes in ohmic resistance. However, samples heated at temperatures above 100^{o}C showed changes in proton conductivity were controlled by both their ohmic resistance and sample thickness. This is important to differentiate since both these processes could be controlled by different mechanisms and changes in material properties to mitigate these issues would need to account for both.

The final conclusion is, in general, the thicker samples displayed increased proton conductivity at the same processing conditions compared to their thinner sample counterparts. Since all three sample types had the same chemical structure this difference in conductivity is hypothesized to result from the increased sample mass which delayed degradation in the sample. It is important to note that, since all other material properties are the same between the samples, these thicker samples would still be expected to reach the same proton conductivities as the thinnest sample, but it would take longer.

These insights and conclusions also point to some important stack design decision and operational changes to consider. First, the formulation of the membrane is important since leaching of different compounds can occur [6] from the membrane into the exhaust has been shown to occur. Previous results have also shown leaching can occur at traditional operating temperatures of 65^{o}C. As demonstrated in this report acetic acid formulated into the membrane should be avoided, but the addition of other acidic compounds should be investigated prior to being used as they may have similar results as well.

Next, heat management of the stack is critical. Not only does thermal degradation of the membranes impact stack performance over time but also can increase the concentration of leached compounds found in the exhaust water. Increasing the concentration of leached components further intensifies the membrane proton conductivity degradation, shown in this paper.

The final recommendation is if temperatures above 100^{o}C are to be used Nafion© of the chemical formulation studied in this paper is not an appropriate material. Modifications to its chemical formulation would need to mitigate increases in ohmic resistance and structural swelling without leaching. This may prove to be a difficult task and the use of a completely different membrane formulation may be required instead.

6. References

[1] W.Bi and T. Fuller, "Temperature Effects on PEM Fuel Cells Pt/C Catalyst Degradation," *J. Electrochem. Soc.,* vol. 155, no. 2, pp. B215-B221, 2008.

[2] H. T. Q. Yan, Y.-W. Lee, K. Liang and H. Causey, "Effect of Sub-Freezing Temperatures on a PEM Fuel Cell Performance Startup and Fuel Cell Components," *J. Power Sources,* vol. 160, pp. 1242-1250, 2006.

[3] R. McDonald, C. Mittelsteadt and E. Thompson, "Effect of Deep Temperature Cycling on Nafion 112 Membranes and Membrane Electrode Assemblies," *Fuel Cells,* vol. 4, no. 3, pp. 208-213, 2004.

[4] J. Gilbert, N. Kariuki, X. Wang, A. Kropf, K. Yu, D. Groom, P. Ferreira, D. Morgan and D. Myers, "Pt Catalyst Degradation in Aqueous and Fuel Cell Environments Studied via In-Operando Anomalous Small-Angle X-Ray Scattering," *Electrochim. Acta,* vol. 173, pp. 223-234, 2015.

[5] R. Kerr, H. Garcia, M. Radtedt, P. Wagner, S. Alfaro, M. Romero, C. Terkelsen, T. Steenberg and H. Hjuler, "Lifetime and Degradation of High Temperature PEM Membrane Electrode Assemblies," *Int. J. Hydrog. Energy,* vol. 40, pp. 16860-16866, 2015.

[6] T. Burye, "Effect of PEM Fuel Cell Exhaust Water Conductivity on Catalyst Degradation using Thermal Degradation Resistant Polymer Membranes," *Int. J. Hydrogen Energy,* vol. 45, no. 20, pp. 11733-11748, 2020.

[7] T. Burye, "Impact of Nafion PEM Fuel Cell Membrane Thickness on Structural Durability while Operated >100°C using In-Situ XRD Characterization," GVSC, 2020.

[8] Y. Sone, P. Ekdunge and D. Simonsson, "Proton Conductivity of Nafion 117 as Measured by a Four-Electrode AC Impedance Method," *J. Electrochem. Soc.,* vol. 143, no. 4, pp. 1254-1259, 1996.

[9] T. Fuller and J. Newman, "Experimental Determination of the Transport Number of Water in Nafion 117 Membrane," *J. Electrochem. Soc.,* vol. 139, no. 5, pp. 1332-1337, 1992.

[10] M. Cappadonia, J. Erning and U. Stimming, "Proton Conduction of Nafion 117 Membrane between 140K and Room Temperature," *J. Electroanal. Chem.,* vol. 376, pp. 189-193, 1994.

[11] K. Mauitz and R. Moore, "State of Understanding of Nafion," *Chem. Rev.,* vol. 104, no. 10, pp. 4535-4585, 2004.

[12] H.-G. Haubold, T. Vad, H. Jungbluth and P. Hiller, "Nano Structure of NAFION: A SAXS Study," *Electrochim. Acta,* vol. 46, pp. 1559-1563, 2001.

[13] V. Noto, R. Gliubizzi, E. Negro, M. Vittadello and G. Pace, "Hybrid Inorganic-Organic Proton Conducting Membranes Based on Nafion and 5 wt% of MxOy (M = Ti, Zr, Hf, Ta, and W) Part I. Synthesis, Properties and Vibrational Studies," *Electrochim. Acta,* vol. 53, pp. 1618-1627, 2007.

[14] V. Noto, R. Gliubizzi, E. Negro and G. Pace, "Effect of SiO2 on Relaxation Phenomena and Mechanism of Ion Conductivity of [Nafion/(SiO2)x] Composite Membranes," *J. Phys. Chem. B,* vol. 110, no. 49, pp. 24972-24986, 2006.

[15] M. Laporta, M. Pegoraro and L. Zanderighi, "Perfluorosulfonated Membrane (Nafion): FT-IR Study of the State of Water with Increasing Humidity," *Phys. Chem. Chem. Phys.,* vol. 1, no. 19, pp. 4619-4628, 1999.

[16] M. Hannon, F. Boerio and J. Koenig, "Vibrational Analysis of Polytetrafluoroethylene," *J. Chem. Phys.,* vol. 50, p. 2829, 1969.

[17] G. Zerbi and M. Sacchi, "Dynamics of Polymers as Structrally Disordered Systems. Vibrational Spectrum and Structure of Poly(tetrafluoroethylene)," *Macromolecules,* vol. 6, no. 5, pp. 692-699, 1973.

[18] G. Masetti, F. Cabassi, G. Morelli and G. Zerbi, "Conformational Order and Disorder in Poly(tetrafluoroethylene) from the Infrared Spectrum," *Macromolecules,* vol. 6, no. 5, pp. 700-707, 1973.

[19] A. Gruger, A. Regis, T. Schmatko and P. Colomban, "Nanostructure of Nafion Membranes at Different States of Hydration: An IR and Raman Study," *Vib. Spectrosc.,* vol. 26, no. 2, pp. 215-225, 2001.

[20] Z. Liang, W. Chen, J. Liu, S. Wang, Z. Zhou, W. Li, G. Sun and Q. Xin, "FT-IR Study of the Microstructure of Nafion Membrane," *J. Membrane. Sci.,* vol. 233, no. 1-2, pp. 39-44, 2004.

[21] T. Blanton and R. Koestner, "Characterization of NAFION Proton Exchange Membrane Films using Wide-Angle X-Ray Diffraction," *International Centre for Diffraction Data,* vol. 9, 2015.

[22] H. Tang, S. Peikang, S. Jiang, F. Wang and M. Pan, "A Degradation Study of Nafion Proton Exchange Membrane of PEM Fuel Cells," *J. Power Sources,* vol. 170, pp. 85-92, 2007.

[23] W. Bi, G. Gray and T. Fuller, "PEM Fuel Cell Pt/C Dissolution and Deposition in Nafion Electrolyte," *Electrochem. Solid State Lett.,* vol. 10, no. 5, pp. B101-B104, 2007.

[24] S. Lee, S. Mukerjee, J. McBreen, Y. Rho, Y. Kho and T. Lee, "Effects of Nafion Impregnation on Performances of PEMFC Electrodes," *Electrochim. Acta,* vol. 43, no. 24, pp. 3693-3701, 1998.

[25] V. Ramani, H. Kunz and J. Fenton, "Investigation of Nafion/HPA Composite Membranes for High Temperature/Low Relative Humidity PEMFC Operation," *J. Membrane Sci.,* vol. 232, pp. 31-44, 2004.

[26] R. Scipioni, D. Gazzoli, F. Teocoli, O. Palumbo, A. Paolone, N. Ibris, S. Brutti and M. Navarra, "Preparation and Characterization of Nanocomposite Polymer Membranes Containing Functionalized SnO2 Additives," *Membranes,* vol. 4, pp. 123-142, 2014.

[27] Q. Yan, H. Toghiani, Y.-W. Lee, K. Liang and H. Causey, "Effect of Sub-Freezing Temperatures on a PEM Fuel Cell Performance, Startup and Fuel Cell Components," *J. Power Sources,* vol. 160, pp. 1242-1250, 2006.